

See discussions, stats, and author profiles for this publication at: <https://www.researchgate.net/publication/276149132>

Detailed Biological Profiling of a Photoactivated and Apoptosis Inducing pdppz Ruthenium(II) Polypyridyl Complex in Cancer Cells

ARTICLE *in* JOURNAL OF MEDICINAL CHEMISTRY · MAY 2015

Impact Factor: 5.45 · DOI: 10.1021/acs.jmedchem.5b00451 · Source: PubMed

CITATIONS

3

READS

78

9 AUTHORS, INCLUDING:



[Robert B P Elmes](#)

National University of Ireland, Maynooth

18 PUBLICATIONS 185 CITATIONS

[SEE PROFILE](#)



[Marialuisa Erby](#)

Royal College of Surgeons in Ireland

6 PUBLICATIONS 52 CITATIONS

[SEE PROFILE](#)



[David Clive Williams](#)

Trinity College Dublin

143 PUBLICATIONS 2,613 CITATIONS

[SEE PROFILE](#)

Detailed biological profiling of a photoactivated and apoptosis inducing pdppz Ruthenium (II) polypyridyl complex in cancer cells

Thorfinnur Gunnlaugsson, Susan M. Cloonan, Robert Elmes, MariaLuisa Erby, Sandra A. Bright, Fergus E Poynton, Derek E. Nolan, Susan Jane Quinn, and D. Clive Williams

J. Med. Chem., Just Accepted Manuscript • DOI: 10.1021/acs.jmedchem.5b00451 • Publication Date (Web): 11 May 2015

Downloaded from <http://pubs.acs.org> on May 13, 2015

Just Accepted

"Just Accepted" manuscripts have been peer-reviewed and accepted for publication. They are posted online prior to technical editing, formatting for publication and author proofing. The American Chemical Society provides "Just Accepted" as a free service to the research community to expedite the dissemination of scientific material as soon as possible after acceptance. "Just Accepted" manuscripts appear in full in PDF format accompanied by an HTML abstract. "Just Accepted" manuscripts have been fully peer reviewed, but should not be considered the official version of record. They are accessible to all readers and citable by the Digital Object Identifier (DOI®). "Just Accepted" is an optional service offered to authors. Therefore, the "Just Accepted" Web site may not include all articles that will be published in the journal. After a manuscript is technically edited and formatted, it will be removed from the "Just Accepted" Web site and published as an ASAP article. Note that technical editing may introduce minor changes to the manuscript text and/or graphics which could affect content, and all legal disclaimers and ethical guidelines that apply to the journal pertain. ACS cannot be held responsible for errors or consequences arising from the use of information contained in these "Just Accepted" manuscripts.



ACS Publications

High quality. High impact.

Journal of Medicinal Chemistry is published by the American Chemical Society. 1155 Sixteenth Street N.W., Washington, DC 20036

Published by American Chemical Society. Copyright © American Chemical Society. However, no copyright claim is made to original U.S. Government works, or works produced by employees of any Commonwealth realm Crown government in the course of their duties.

1
2
3
4 Detailed biological profiling of a photoactivated
5
6 and apoptosis inducing pdppz Ruthenium(II)
7
8 polypyridyl complex in cancer cells
9
10
11
12
13

14
15
16
17
18 Suzanne M. Cloonan^{1†}, Robert B. P. Elmes^{2‡}, MariaLuisa Erby¹, Sandra A. Bright¹, Fergus
19
20 E. Poynton², Derek E. Nolan¹, Susan J. Quinn³, Thorfinnur Gunnlaugsson², D. Clive
21
22 Williams¹
23
24

25 ¹School of Biochemistry and Immunology and Trinity Biomedical Sciences Institute, Trinity
26 College Dublin, Dublin 2, Ireland. ²School of Chemistry and Trinity Biomedical Sciences
27 Institute, Centre for Synthesis and Chemical Biology, Trinity College Dublin, Dublin 2,
28 Ireland. ³School of Chemistry and Chemical Biology, University College Dublin, Dublin 2,
29 Ireland.
30
31
32
33
34
35
36

37 KEYWORDS Photodynamic therapy, cancer, Ruthenium, imaging agents
38
39

40 ABSTRACT Ruthenium polypyridyl complexes show great promise as new photodynamic
41 therapy (PDT) agents. However, a lack of detailed understanding of their mode of action in
42 cells poses a challenge to their development. We have designed a new Ru(II) PDT candidate
43 which efficiently enters cells by incorporation of the lipophilic aromatic pdppz ([2, 3-
44 h]dipyrido[3,2-a:2',3'-c]phenazine)) ligand, and exhibits photoactivity through incorporation
45 of 1,4,5,8-tetraazaphenanthrene ancillary ligands. Its photoreactivity towards biomolecules
46 was studied *in vitro*, where light-activation caused DNA cleavage. Cellular internalization
47 occurred *via* an energy dependent mechanism. Confocal and transition electron microscopy
48 revealed that the complex localises in various organelles, including the mitochondria. The
49
50
51
52
53
54
55
56
57
58
59
60

1 complex is non-toxic in the dark, with cellular clearance within 96 hours, however upon
2 visible light-activation it induces caspase- and reactive oxygen species-dependent apoptosis,
3 with low micromolar IC₅₀ values. This investigation greatly increases our understanding of
4 such systems *in cellulo*, aiding development and realisation of their application in cancer
5 therapy.
6
7
8
9
10
11
12
13
14
15
16
17
18
19
20
21
22
23
24
25
26
27
28
29
30
31
32
33
34
35
36
37
38
39
40
41
42
43
44
45
46
47
48
49
50
51
52
53
54
55
56
57
58
59
60

Introduction

The excellent photophysical properties of Ru(II) polypyridyl complexes have been intensely investigated over the past 30 years with a view to varied applications¹. The biological activity of Ru(II) complexes has been investigated since the early 1950's when Dwyer and co-workers reported their antibacterial activity. Since then a number of complexes have been developed as potential anti-cancer agents²⁻⁴. In particular, their DNA binding affinity and photo-triggered DNA damage has presented them as potential cellular imaging and therapeutic agents⁵⁻¹². The advantages of using such Ru(II) polypyridyl complexes as cellular targeting agents lies in the fact that the structural nature of the polypyridyl units will dictate the overall function of the metal complex, which includes their solubility, lipophilicity, charge, and importantly, their photophysical properties. The use of extended polypyridyl ligands suchs as dipyrido[3,2-a:2',3'-c]phenazine (dppz) allows strong binding to DNA through intercalation⁴. The $[\text{Ru}(\text{phen})_2\text{dppz}]^{2+}$ (phen = 1,10-phenanthroline) acts as a light-switch complex, which is non-luminescent in solution but luminesces strongly when bound to DNA which can be applied to DNA imaging. Recently, Ru(II) complexes developed by us and others^{13, 14} have been shown to act as effective cellular imaging agents without giving rise to cellular photodamage. Kelly *et al.*, have shown that $[\text{Ru}(\text{TAP})_2\text{dppz}]^{2+}$ (TAP = tetraazaphenanthrene) which contains π -deficient, electron accepting ligands, causes photodamage of DNA through oxidation of guanine¹⁵⁻¹⁷. The related complex $[\text{Ru}(\text{TAP})_2\text{bpy}]^{2+}$ has been shown to cause DNA-damage through photo-adduct formation(30). Recently, crystallographic resolution of enantiopure Ru(II)(dppz) complexes bound to DNA sequences has been achieved by Kelly, Cardin and co-workers^{5, 11} and Barton¹⁸ and co-workers. These structures have provided detailed structural understanding of the binding interactions that give rise to the light-switch and photodamage phenomena.

Photodynamic therapy (PDT) is a well-recognised tumour ablative modality for the efficacious treatment of various cutaneous and deep tissue tumours¹⁹. PDT involves the administration of a ‘photosensitiser’ either systemically or locally and subsequent

illumination with a low energy, tissue-penetrable light. The interaction of the photosensitiser and light results in the photochemical activation of molecules within the cell (usually the production of activated oxygen species) which results in its rapid destruction. The ideal photosensitiser should be water-soluble, easily accumulate in a cancer cell, should possess no or very low dark toxicity and be non-mutagenic²⁰. Importantly, it should be readily available and be able to induce programmed cell death. The majority of PDT agents developed to date have been porphyrin-based and as a result suffer from a number of undesirable characteristics: hydrophobicity, poor light absorption, lack of specificity, dark toxicity and prolonged skin sensitivity to name but a few²¹. Ru(II) polypyridyl complexes have recently been recognised as a major class of ‘new’ types of PDT agents that can overcome some of the above problems.^{22,23} While such systems often possess higher energy absorptions than that seen for porphyrin-based systems, then these can often been ‘pushed’ to longer wavelengths by ligand design, or by using two-photon excitation, the latter enabling the addressing of the excited state properties of the complexes at comparable or longer wavelengths than currently use in the clinic.

Interestingly, while a number of Ru(II) based complexes have been shown to successfully induce DNA photocleavage following light activation *in vitro*^{2, 7, 22, 23} only a limited number of such complexes have shown promise as potential PDT agents by demonstrating photo-activation induced-cytotoxicity at a cellular level^{3, 12, 24}, whilst there has only been one report to date into the biological mechanism of action of cell death behind such Ru(II) polypyridyl complex-induced PDT within cells²⁵. It is clear that in order to realise the therapeutic and diagnostic potential of these complexes a thorough understanding of the internalisation properties and activity is essential. Ideally, this requires mapping the path from uptake, to localisation, to activity and toxicity and finally the means and extent of clearance, and while a number of studies have explored individual aspects, a full picture has yet to be captured. Thomas and co-workers have demonstrated that various Ru(II) polypyridyl complexes can be taken up into cells by non-endocytotic active transport. Using non-

cytotoxic Ru(II) complexes, the group showed that such complexes could accumulate within cells and directly image nuclear DNA²⁶. Indeed, a dinuclear Ru(II) polypyridyl compound was found to enter living cells, accumulated in the nucleus (and other organelles) and could directly image nuclear DNA utilising the MLCT ‘light-switch’ property of the compound. Several other researchers have shown similar effects, but often the delivery of such complexes has required the use of structures possessing polyamino acid conjugates as delivery vehicles²⁷⁻³⁰.

In this study we report a comprehensive profile of the biological activity of a new Ru(II) polypryridyl anti-cancer phototherapy agent, [Ru(TAP)₂pdppz]²⁺ (pdppz = [2, 3-h]dipyrido[3,2-a:2',3'-c]phenazine) **5**. The key design features of this complex are the combination of (a) an extended ‘hooked’ dipyridophenazine ligand for enhanced intercalation and DNA binding with (b) a π -deficient ligand network for photo-triggered damage. In addition, we present results for the control complex [Ru(phen)₂pdppz]²⁺ **4** which also possesses the ‘hooked’ dipyridophenazine ligand but is not expected to cause significant photodamage due to the absence of the TAP ligands. Rapid cellular uptake of these complexes, followed by localisation within mitochondria is observed. This is followed by perinuclear clustering of the mitochondria, which results in changes in cellular appearance with the formation of a concave or bean-shaped nucleus. **5** is found to give rise to minimal dark toxicity and recovery of the cell upon removal and elimination of the complex. Then, upon photoactivation, programmed cellular death is turned on leading to rapid cellular death. Furthermore, we demonstrate part of the mechanism of action of this novel Ru(II) PDT agent.

Results and Discussion

Synthesis and spectral characteristics of Ru(II) complexes: The ligands and Ru(II) complexes employed in the present studies are shown in Figure 1a. In the design of **4** and **5**, we anticipated that further extension of the flat, planar well known dppz structure³¹ would increase DNA binding ability; which would be concomitantly felt in modulation of their

photophysical properties. This was informed from our recent study of the interaction of the quaternarised pdppz ligand with DNA³¹. In the case of **5** it was envisaged that incorporation of a ‘TAP-like’ moiety on the ligand in tandem with variation of the ancillary ligands would confer both increased DNA binding and photocleavage ability with possible formation of DNA – photoadducts, as has been seen previously with Ru(II) complexes containing TAP ligands^{32, 33}. The synthetic pathway of **4** and **5** is shown in Figure 1a (see Supplementary Information for experimental data). In short, the synthesis of **3** was achieved by condensation of 5, 6 diaminoquinoxaline³⁴ **1** with 1, 10-phenanthroline-5,6-dione^{31, 35} **2** by reflux in EtOH yielding **3** as a grey solid in 95% yield. The microwave irradiation of **3** in the presence of the appropriate ruthenium bispolypyridyl dichloride³⁶ for 15 min followed by precipitation from water using excess ammonium hexafluorophosphate yielded the crude complexes **4** and **5** in 69% and 52% respectively after purification. Synthesised as their chloride salts, all complexes are water-soluble, and their photophysical properties were investigated in 10 mM phosphate-buffered aqueous solutions at pH 7.4.

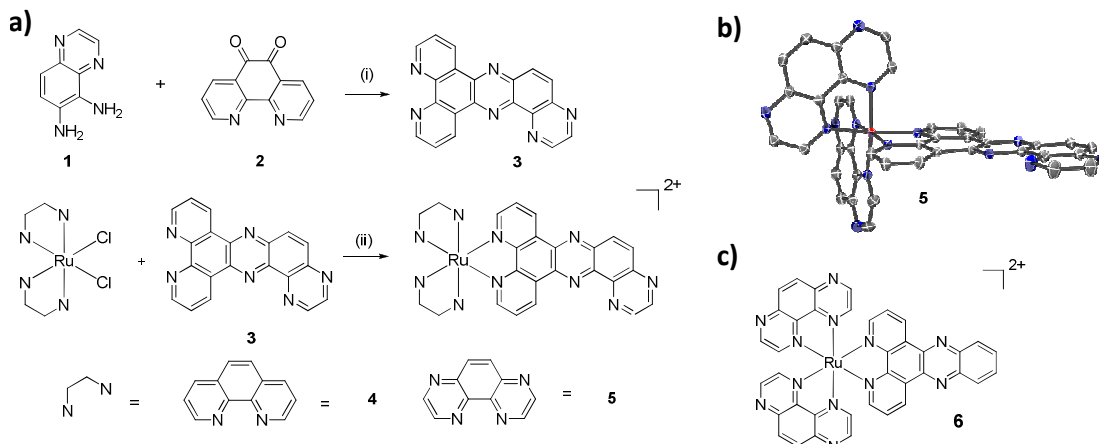


Figure 1: (a) Synthesis of **3** (free ligand) and corresponding Ru(II) complexes **4** and **5**. (i) glyoxal, EtOH, reflux (ii) H₂O, 50W. (b) The X-ray crystal structure of **5**. PF₆⁻ counterions and solvent molecules are omitted for clarity (see supplementary information for full structure), ellipsoids are shown at 40% probability. (c) The chemical structure of **6**.

Red prism shaped crystals were obtained of the hexafluorophosphate complex of **5** by slow evaporation from acetonitrile. The X-ray crystal structure of **5** is shown in Figure 1b and confirms the incorporation of two TAP ligands and the extended planar pdppz ligand around the Ru(II) centre. The complex crystallised in a triclinic system with space group P₁ and the unit cell contains two complexes (the delta and lambda enantiomers) and four hexafluorophosphate counteranions. Complex **5** exhibits a distorted octahedral geometry, with Ru – N bond distances lying in a narrow range between 2.060(3) - 2.086(3) Å. [Ru(TAP)₂dppz]²⁺, **6**, was synthesised according to a modification of the literature procedure reported by Kirsch-De Mesmaeker *et al.*,²³ and its chemical structure is shown in Figure 1c.

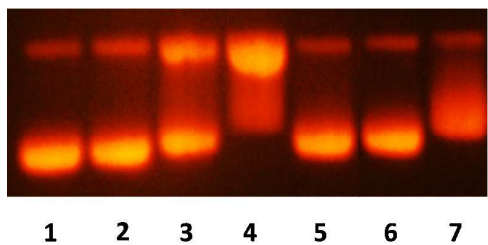
The characteristic UV-Vis absorbance spectra, together with the excitation and emission spectra of **4** and **5** are shown in the Supplementary Information, showing transitions that are typical of related compounds such as dipyrido[3,2-a:2',3'-c]phenazine (dppz). **5** possesses a band at 308 nm due to the pdppz ligand and a broad structured band centred at 415 nm which is attributed to the MLCT transitions of the Ru(II) centre. Excitation of **5** at 415 nm in aqueous pH 7.4 buffered solution, gave rise to MLCT based emission with λ_{max} at 630 nm. This is similar behaviour to that observed for Ru(TAP)₂(dppz)²³ which can be justified if the lowest excited MLCT state is due to a charge transfer to one of the two TAP ligands. As expected, no MLCT based emission was observed for the control complex **4**.

In the first step to profile the biological activity of **5** the DNA binding affinity was investigated. A series of DNA titrations were carried out in 10 mM phosphate buffer at pH 7.4. The addition of salmon testes (st) DNA to **4** and **5** resulted in significant changes to their absorption spectra which are summarised in Supplementary Information. These showed that in the case of **4** a 53% hypochromism was observed for the pdppz band (located at 308 nm), while the MLCT band experienced a 30% hypochromism. For structure **5**, a hypochromism of 43% and 30% was seen for these two transitions, respectively. These defined hypochromicities would indicate intercalation of the pdppz ligand between the stacked bases.

The intrinsic binding constant (**K**) and binding site stoichiometry (**n**) were determined from these spectroscopic results using the model of Bard *et al.*,³⁷ (see Supporting Information), which showed that **4** and **5** had high affinity for DNA, with **K** = $1.2 \times 10^7 \text{ M}^{-1}$ (± 0.3) and **n** = 1.45 (± 0.03) for **4**, while for **5** **K** = $5.4 \times 10^6 \text{ M}^{-1}$ (± 0.5) and **n** = 1.55 (± 0.02). In the presence of 100 mM NaCl, the resulting **K** values were found to be in the region of 10^6 M^{-1} (Supplementary Information) indicating that binding strength is only moderately sensitive to salt concentration. In agreement with the ground state studies, significant changes were also seen in the emission spectra of **4** and **5** upon binding to DNA (See Supplementary Information). Compound **4** is best described as a ‘light-switch’ for DNA as it showed no significant luminescence in aqueous buffer solution (as has been demonstrated for other phen based polypyridyl Ru-complexes containing one or more dppz structures) as upon addition of st-DNA, intense MLCT-based photoluminescence was observed, centred at 620 nm (Supplementary Information). Complex **5** exhibits opposite behaviour upon addition of st-DNA; where the intense luminescence of **5** in aqueous buffer is effectively quenched upon addition of DNA, behaviour which is also characteristic of the excited MLCT Ru-TAP state where the excited state is localised on the TAP ligand. $[\text{Ru}(\text{TAP})_2(\text{L})]^{2+}$ complexes (L = phen or bpy)^{16, 38}, have been shown to photo-oxidise guanine containing nucleotides. Therefore the emission of **5** was next investigated in the presence of $[\text{poly}(\text{dA-dT})]_2$ and $[\text{poly}(\text{dG-dC})]_2$.[§] For the former, a marked 57% increase in the MLCT emission intensity was observed; induced by the protection afforded upon intercalation into the double helix from oxygen based quenching. Conversely, in the case of $[\text{poly}(\text{dG-dC})]_2$, a dramatic 98% luminescence decrease was observed most likely due to the aforementioned photooxidation process. Analysis of the binding of these complexes by Linear Dichromism (LD) spectroscopy further supported the intercalative nature of binding of both complexes to DNA (See Supplementary Information).

Having demonstrated the high affinity of **5** for DNA we next considered the DNA photo cleavage ability of the complex. In order to evaluate this for **4** and **5**, agarose gel

1 electrophoresis of pBR322 plasmid DNA was undertaken (Fig.2). When incubated in the dark
2 neither complex showed any DNA cleavage. However, **5** showed extremely efficient
3 photocleavage after 30 min irradiation under aerobic conditions at a DNA phosphate to
4 Ru(II) dye (P/D) ratio of 100. Furthermore at P/D = 50 the complex showed complete
5 conversion of the supercoiled DNA to both nicked and linear forms. As expected, complex **4**
6 did not show a marked increase in the formation of either linear or nicked DNA strands.
7
8
9
10
11
12
13



24 **Figure 2:** Agarose gel electrophoresis of pBR322 DNA (1 mg/ml) after irradiation (2 J cm^{-2})
25 at $\lambda > 390 \text{ nm}$ in 10 mM phosphate buffer, pH 7. 4; Lane 1: Plasmid DNA control; Lane 2:
26 $[\text{Ru}(\text{bpy})_3]^{2+}$ (P/D 100); Lanes 3-4: **5** (P/D 100, 50); Lane 5 : **5** in the dark (P/D 100); Lanes
27 6-7: **4** (P/D 100, 50).

36 Cellular uptake of Ru(II) polypyridyl complexes

37 The uptake and cellular localisation of **4** and **5** in the dark (no photoactivation) in a cervical
38 cancer cell line (HeLa) was investigated. Confocal fluorescence microscopy was used to
39 track the red-emission arising from the complexes¹⁸ over a period of 4, 8, and 24 h.
40 Complexes appeared to move from the outside of the cell toward the nucleus in a time-
41 dependent manner. Here discrete ‘packets’ of luminescence in the cytoplasm were observed
42 at all time-points with complex **4** and at short time points (4 h) for complex **5**. A large single
43 intense luminescent spot (at the resolution of confocal microscopy) was observed after 8 h
44 associated near the nucleus for complex **5** as demonstrated in Figure 3a. Concomitant with
45 this single location was the observation of a concave or bean-shaped nucleus. After 24 h
46 compound **5** appeared to localise around the nucleus. An enlargement of a representative cell
47
48
49
50
51
52
53
54
55
56
57
58
59

treated with **5** is shown for illustrative purposes in Figure 3b. It should be noted that the difference between the emission properties of **4** and **5** could account for the lower visualisation of **4** in the cytoplasm at earlier time-points. The fact that cellular uptake was found to be temperature-dependent suggests that these compounds are not membrane-permeable and require active or facilitated uptake (Fig.3c).

The control compound **6** was similarly observed to localise in the cytoplasm of HeLa cells, however uptake appeared to be slower with the compound only clearly visible within cells after 24 h. Previous studies have shown that extending the size of the polypyridyl ligand confers lipophilic character to the complexes and results in enhanced uptake into cells^{2, 18} (Supplementary Information).

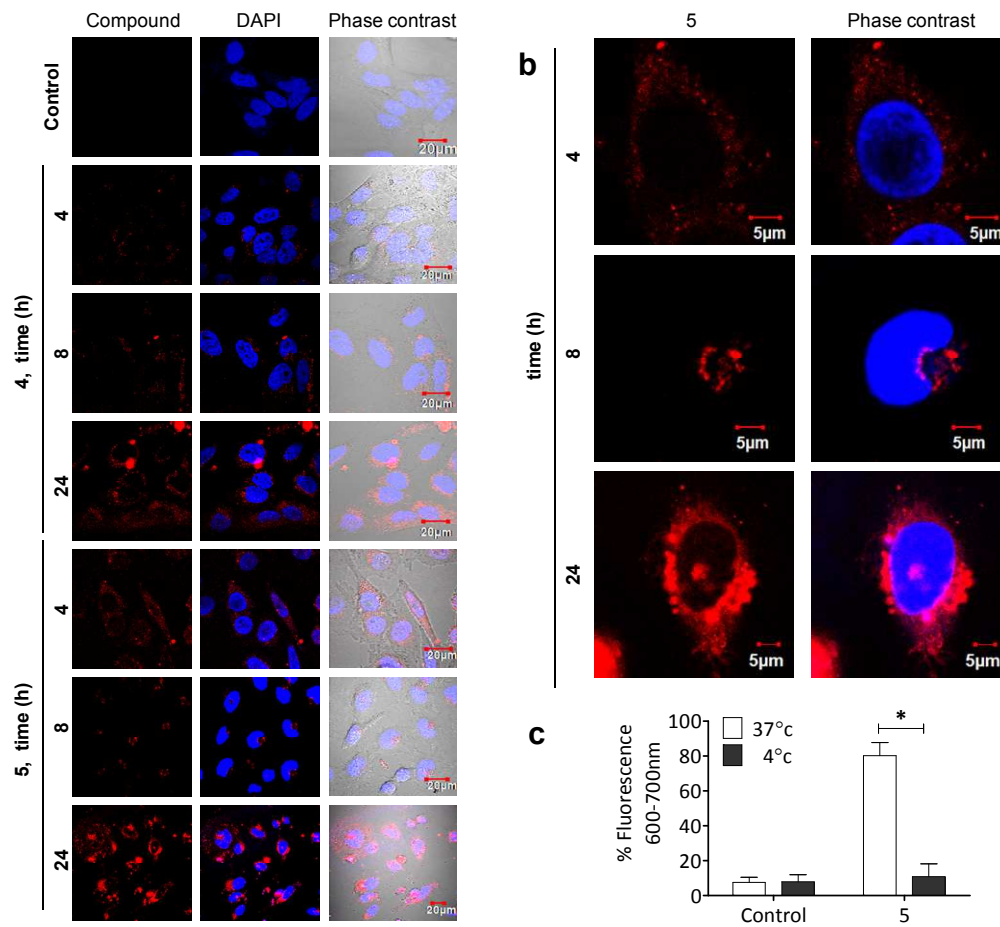


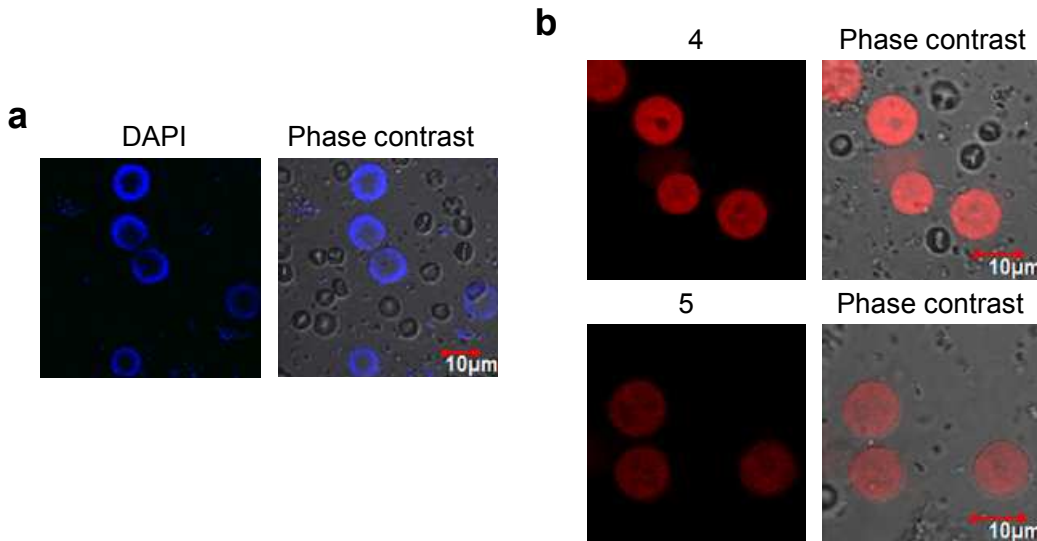
Figure 3: Time dependent localisation of **4** and **5** in HeLa cells. 0.5×10^5 HeLa cells were treated as required, washed twice, incubated with DAPI (Blue nuclear stain) and viewed

1 using an Olympus FV1000 point scanning microscope with a 60x oil immersion lens with an
2 NA of 1.42. (a) Cells were treated with 100 μ M 4 or 5 for 4, 8 or 24 h. (b) Cells were
3 treated with 100 μ M 5 for 24 h; enlargement of representative cells for illustrative purposes.
4
5 (c) Cells were treated with 100 μ M 5 for 4 h at 37 °C or 4 °C and the percentage of cells with
6 compound fluorescence was expressed over the total amount of cells (approximately 50) per
7 field of view. Data points represent the mean \pm S.E.M.
8
9
10
11
12
13
14

15 Uptake of compounds into isolated organelles

16

17 As these compounds were shown to bind to st-DNA, but did not appear to localise within the
18 nucleus of whole cells, organelles were isolated from rat liver tissue and incubated for 20 min
19 with complexes 4 and 5. Both compounds were shown to be taken up by isolated, intact
20 nuclei (Fig. 4a-b). Compound 5 was shown to have a decreased luminescence intensity when
21 compared with compound 4, as was predicted based on the observed quenching of 5 when
22 bound to DNA, as discussed above. The compounds stained the nucleus in a similar manner
23 to DAPI.

24

52 **Figure 4:** Rat liver nuclei show uptake of compounds 4 and 5. Nuclear-rich fractions isolated
53 from rat liver tissue were treated with 100 μ M of compound 4 or 5 for 20 min before
54
55
56
57
58
59
60

organelles were washed with PBS and viewed by confocal microscopy. Isolated nuclei stained with (a) DAPI and (b) Ru(II) complex 4 or 5.

Investigation into the subcellular localisation and light activation of compounds 4 and 5

The results listed above confirm the ability of the compounds to bind not only to isolated st-DNA, but also to bind to DNA in its natural environment within a mammalian nucleus. However, when these complexes are incubated with whole cells the compounds fail to reach the nucleus. In order to investigate why this occurred we looked at the subcellular localisation of the compounds in whole cells using confocal fluorescence microscopy and examining the co-localisation of **5** with mitochondria (Fig.5a), lysosomes (Fig.5b) and the endoplasmic reticulum (Fig.5c). The results of these experiments suggest that **5** appears to co-localise to mitochondria and/or lysosomes (Fig.5a-d).

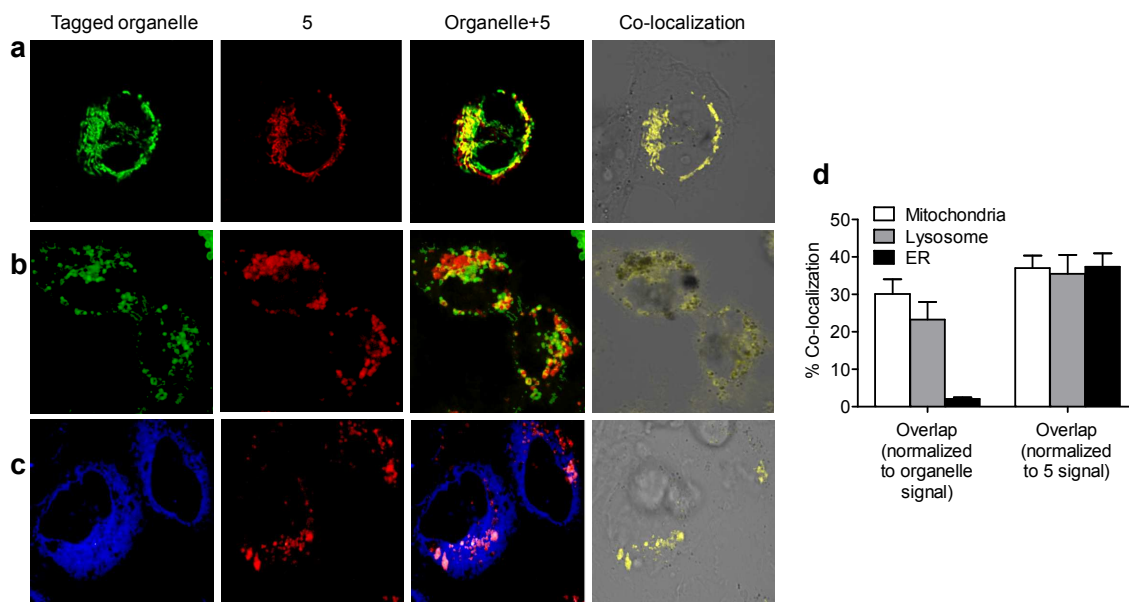


Figure 5: Sub-cellular location of **5**. Assessment of co-localisation of **5** with mitochondria (**a,d**), lysosomes (**b,d**) and endoplasmic reticulum (ER) (**c,d**).

Further analysis of Ru(II) complex localisation using transmission electron microscopy (TEM) of HeLa cells revealed that **5** accumulates in mitochondria as indicated by the dense staining of HeLa cell mitochondria treated with **5** (Fig.6a). Previously, dinuclear Ru(II) polypyridyl complexes prepared by the Keene group have been observed to also accumulate in the mitochondria³. The TEM imaging experiments also confirm the clustering of loaded mitochondria near the nucleus, also known as perinuclear mitochondrial clustering. Compound **5** was also shown to reduce the mitochondrial membrane potential (MMP) of HeLa cells *in vitro* after 30 min, but with apparent recovery after 4 h, showing the reduction in MMP to be time-dependent and further confirming the accumulation of **5** in mitochondria

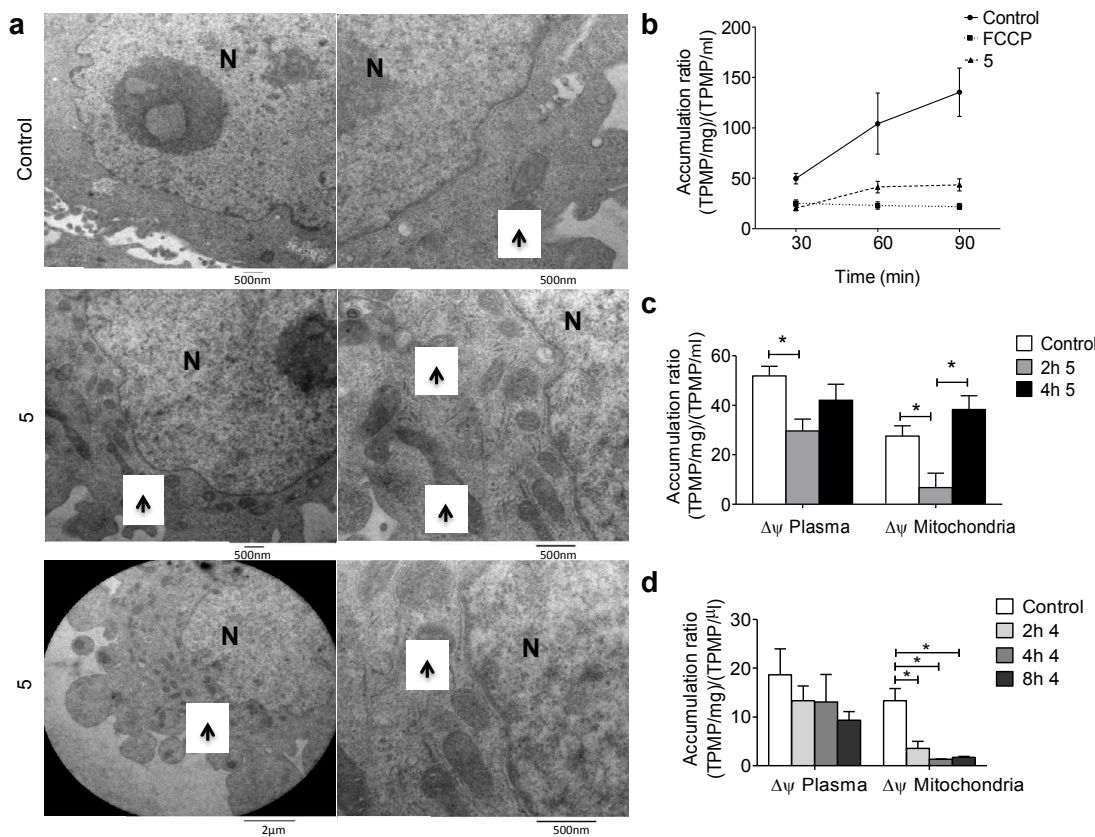


Figure 6: The effect of Ru(II) complexes on mitochondria. TEM of HeLa cells untreated (Control), or treated with 100 μ M **5** at different magnifications. The effects of **5** (**b**, **c**) and **4** (**d**) on TPMP accumulation, a direct measure of MMP. N – nucleus, arrowheads – mitochondria. Statistical analysis was performed using a one-way ANOVA, *, p < 0.05. Data points represent the mean \pm S.E.M.

(Fig.6b,c). Compound **4** also reduced the MMP of HeLa cells (Fig.6d) but unlike that seen for **5** above, without recovery even after 8 h.

In order to evaluate the cytotoxic anticancer potential of **4** and **5**, both were tested for cytotoxicity in five cancer cells lines; two mesothelioma cell lines, the cervical cancer cell line, HeLa and two Burkitt's lymphoma cell lines. As these complexes could potentially exhibit 'light-switch' cytotoxicity inside the cells upon light activation, both compounds were 'photoactivated' using low intensity light ($\lambda \geq 400$ nm, $\sim 18 \text{ J cm}^{-2}$) upon incubation in cells and assessed. Of the two complexes, **4** showed no light dependent cytotoxicity at high concentrations in the various cell lines (Table 1). In contrast to these results, compound **5** displayed light-dependent cytotoxicity in HeLa and mesothelioma cells (CRL5915) in a concentration dependent manner (Table 1) with minimal dark toxicity which was observed

Table 1: The effects of Ru(II) complex **4** and **5** on malignant cell lines with or without light activation.

1.5×10^3 cells/well were seeded in a 96-well plate and treated with the respective drug for 24 h \pm irradiation with 18 J cm^{-2} of light. After 24 h, each well was then treated with 20 μl of Alamar Blue and left to incubate at 37°C in the dark for 4-6 h. Fluorescence was read using at 590 nm (excitation 544 nm). The background fluorescence of the media without cells + Alamar Blue was taken away from each group, and the control untreated cells represented 100% cell viability. Data represents the mean \pm S.E.M.

IC₅₀ (μM)	4 - Dark	4 - Light	5 - Dark	5 - Light
HeLa	> 100	>100	70 ± 6.3	8.8 ± 2.9
CRL 5915	73.3 ± 17.7	92.3 ± 19.2	> 100	42.8 ± 2.6
One58	53.2 ± 11.5	62.2 ± 9.3	> 100	38.3 ± 5.6
Mutu-I	> 100	> 100	40.2 ± 3.5	17.6 ± 1.4
DG-75	> 100	90 ± 13.8	> 100	42.5 ± 0.8

only at higher concentrations. These results demonstrate that the activity of the complex is achieved by simple light activation as is clear from determining the IC₅₀ values for the cytotoxicity of **5** in these cell lines when exposed to light which were found to be between 8.8 μM and 43 μM, compared to the IC₅₀ values of between 40.2 μM and greater than 100 μM for the cell lines tested for the cytotoxicity of **5** in the dark. The low cytotoxicity observed for **4** suggests that this complex may be used as a luminescent cellular probe within these cell lines, whereas complex **5** may have more applications as a novel PDT agent. This clearly demonstrates the enormous scope that such complexes have within biology, where simple structural modifications can dictate the function of the resulting Ru(II) polypyridyl complex. The control **6**, was also assessed for light activation and these results demonstrated comparable photo-induced toxicity to **5** (Supplementary Information).

Photo-activation of **5** (100 μM) *in vitro* was monitored using real-time confocal microscopy (image taken every 10 min for 12 h) resulted in cells with an apoptotic phenotype. Using light irradiation alone, in the absence of compound **5**, or by using compound **5** alone in the absence of light irradiation, there was no effect on HeLa cells. Photoactivated cell death was also found to be time-dependent as demonstrated in Figure 7a. Further analysis of the mechanism of cell death elicited by this compound using PI (propidium iodide) FACS (fluorescent activated cell sorter) analysis, which detects the formation of apoptotic bodies, revealed the induction of light-induced apoptosis in a dose- and time-dependent manner, shown in Figure 7b and 7c, respectively. Light-induced cell death was rapid and potent (70-80% cell death at 100 μM) with the dark death effect being minimal (6-8% cell death at 10 and 100 μM). Recent investigations into the anticancer effects of Ru(II) polypyridyl complexes document IC₅₀ values of between 5 μM and 500 μM in the absence of light, implying a weak ‘dark’ toxic effect³⁹. Other Ru(II) complexes have been previously examined as PDT agents, with Ru(II) phthalocyanine, Ru(II)-2,3-

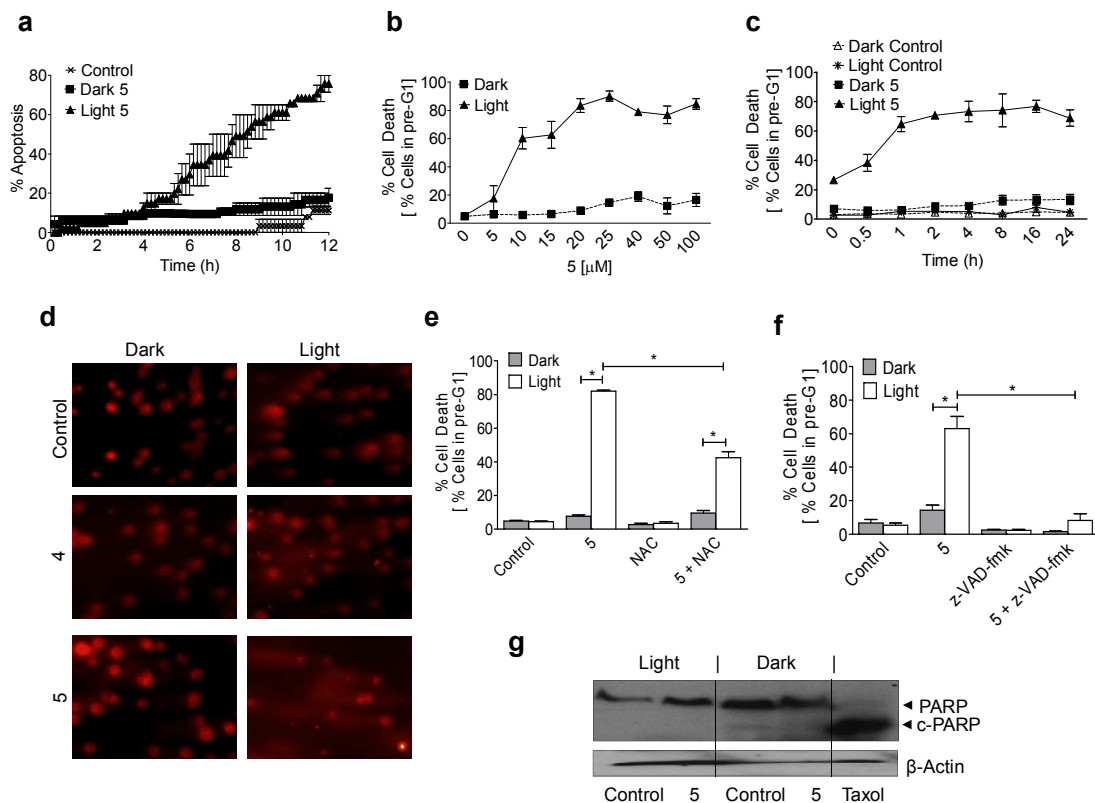


Figure 7: *Ru(II) complex 5 induces programmed cell death of HeLa cells.* $1-5 \times 10^3$ cells/well were seeded and treated with the respective drug for 24 h \pm irradiation with $\sim 18 \text{ Jcm}^{-2}$ of light followed by incubation for the indicated time-points or a further 24 h. Confocal microscopy was used to assess cells for the appearance of apoptotic cells (a). PI staining was used to assess the effect of concentration (b), time (c), ROS inhibition (e) and caspase inhibition (f) on *Ru(II) complex 5* light-induced toxicity. Intracellular DNA strand breakage as identified via the comet assay (d) and cleavage of the enzyme PARP, as identified through western blotting (g) following treatment with 5. Statistical analysis was performed using a one-way ANOVA, *; $p < 0.05$. Data points represent the mean \pm S.E.M.

naphthalocyanines having been shown to display phototoxicity in the low micromolar range^{30, 40} which is comparable to that found in the present study. Previous literature on the efficacy of non-porphyrin PDT agents report IC₅₀ values of between 63 nM and 8 μM in the light compared to between 27 μM and $>100 \mu\text{M}$ in the dark^{41, 42}.

In our study, cells treated with **5** and light irradiation showed a significant degree of single stranded DNA migration and damage compared to dark controls as demonstrated by the single cell gel electrophoresis comet assay (Fig.7d). Cells treated with **4** and irradiation also underwent a small amount of DNA damage, however, this was in no way to the same extent as was observed for **5**-treated cells, as illustrated by shorter comet tails.

As some other PDT agents elicit their cell death effects through the activation of reactive oxygen species (ROS), we utilized the antioxidant *N*-acetyl cysteine (NAC), to investigate the involvement of ROS in photo-induced programmed cell death mediated by **5**. HeLa cells pre-incubated with NAC (5 mM) for 1 h, treated with **5** and activated with light were not found to undergo the same amount of cell death as those cells without NAC as illustrated in Figure 7e. These results suggest that ROS are involved in the photo-induced cell death and that complex **5** may induce a ‘classical’ PDT response in cells as observed with other PDT agents. The involvement of ROS, which are formed in mitochondria, again supports the involvement of **5** with mitochondria. However, it is important to point out that non-oxygen dependent photoreaction pathways of Ru(II) (TAP) complexes with biomolecules have also been reported^{43, 44}.

The cell death induced by **5** was inhibited by pre-treating the cells for 4 h with 40 µM of the general caspase inhibitor z-VAD-fmk (Fig.7f). Caspases are intracellular cysteine proteases involved in forms of programmed cell death and these results further confirmed the cells were undergoing apoptosis that was light induced. Caspases are sometimes known to cleave the DNA repair enzyme PARP (poly(ADP-ribose) polymerase) from a 113 kDa molecule into 89 and 24 kDa fragments during apoptosis. However, this was not found to be the case with **5** as no induced PARP cleavage was observed (Fig.7g). Treatment with paclitaxel was used as a positive control for PARP cleavage. These overall results clearly demonstrate the importance of the presence of the TAP ligand in **5**, which is absent in **4**, and the direct mechanistic effect **5** has on cellular viability. Finally, the ability of a photosensitiser

1 to enter a cell and be eliminated without harming the cell is essential for any effective PDT
2 agent. In this study we examined the effects of **5** on HeLa cells over a 48-96 h time frame
3 using PI FACS analysis and confocal microscopy. Confocal microscopy demonstrated that
4 after 48 and 96 h, **5** is no longer visible in the cell. PI FACS analysis also showed that **5** had
5 no obvious apoptotic effect after 48 h theoretically reducing any potential side effects *in vivo*
6 (Supplementary Information). Collectively, these results support the clinical advancement of
7 complex **5** as a potential PDT agent. This complex will be used as a platform for the
8 development of improved structures with higher wavelength absorptions and improved
9 efficacy. A higher absorption wavelength would eliminate any absorption by haemoglobin or
10 other blood proteins *in vivo* and could also be achieved by using two photon microscopy
11 instead of conventional confocal (or one photon) microscopy, while still maintaining the
12 same emission spectrum as recently demonstrated with similar Ru polypyridyl compounds⁴⁵
13
14⁴⁷. Also of clinical importance, Ruthenium compounds are known to bind to high and low
15 density lipoproteins, serum proteins and albumin *in vivo*, which have been shown to
16 enhance drug accumulation into the tumour tissue^{48, 49}, interestingly however, a recent study
17 by Pernot *et al.*, on arene ruthenium porphyrin PDT compounds demonstrated that fluence
18 rate in PDT was more important than the photosensitiser concentration⁵⁰. Conventional
19 chemotherapy targets rapidly dividing cells as opposed to tumour cells resulting in serious
20 side-effects, and while targeted therapies overcome this limitation, they are expensive and
21 only available for a limited number of cancers with specific, well defined mutations. In
22 contrast, the potential use of complex **5** as a PDT agent would overcome these obstacles as
23 the very nature of PDT agents ensures that only complexes at the site of interest, a tumour,
24 would be photo-activated to induce cell death *in vivo*. Whilst, non-tumour cells found in the
25 tumour region would also likely experience PDT-induced toxicity, the lack of toxicity with
26 non-photoactivated complexes found in the rest of the body together with the observed
27 clearance of non-photoactivated complexes from healthy HeLa cells, also highlights the
28 development potential of complex **5**.

Conclusion

In this study, we report the synthesis of a new photodynamic therapeutic agent **5** and the related control pdppz light-switch complex **4**. The luminescence of **4** significantly increases when bound to DNA while the luminescence of **5** decreases when bound to DNA. While the structures of **4** and **5** are similar, they have very different mechanisms of action on st-DNA in aqueous solution. While both compounds have been shown to bind DNA with high affinity, gel electrophoresis measurements reveal that only complex **5** cleaves DNA. We further demonstrate that the presence of the TAP ligand in **5** is instrumental to the photo-activity of the complex within cells (this we also show to be the case for **6**). From our thorough investigation of the biological properties of these complexes, a number of important observations have been made, including that the complexes are found to be actively transported to the interior of the cells and accumulate with clear visualisation (600 – 700 nm range) within the cells after 8 h. Furthermore, the increased lipophilicity of the extended pdppz ligand employed in **4** and **5⁵¹**, is found to increase the rate of uptake of the complexes compared to the corresponding dppz containing complex **6**. Moreover, the uptake of the complexes **4** and **5** into isolated nuclei indicates that the complexes are capable of displaying MLCT luminescence when bound to DNA within the nuclei; our results confirming that **4** is more emissive compared to **5**, as seen for the binding of these complexes to isolated st-DNA. However, in live cell imaging, the compounds are found to mostly localise within mitochondria and lysosomes, with lesser amounts found in other organelles such as the endoplasmic reticulum. These results clearly highlight the influence the microenvironment of the cell has on the complexes and the importance of performing such experiments in live cells. Further evidence for the mitochondrial localisation of **5** was obtained by TEM studies of HeLa cells, which show densely stained mitochondria appearing to localise around the nucleus. Being lipophilic and cationic in nature, we demonstrate that the complexes enter mitochondria, most likely driven by the MMP; with **5** being shown to reduce the MMP within 30 min of treatment with recovery of the MMP after 4 h. The subsequent perinuclear

1 clustering of compound laden mitochondria may be suggestive of a large degree of
2 depolarisation induced mitophagy as described by Youle *et al.*,⁵².
3

4 The cellular photo-reactivity of **5** was investigated by assessing the
5 antiproliferative/cytotoxicity in the presence and absence of light irradiation of low intensity
6 (18 J cm^{-2}) in a number of malignant cell lines. The complex showed potent light-dependent
7 toxicity in a range of cell lines (IC_{50} values of between $8.8 \mu\text{M}$ and $43 \mu\text{M}$) and was shown to
8 induce dose and time dependent programmed cell death in HeLa cells, the critical
9 involvement of caspases confirmed this form of programmed cell death to be apoptosis. This
10 could be occurring via an electron transfer mechanism (which is photo-induced driven);
11 which could potentially involve binding of **5** to DNA within the mitochondrion itself, though
12 further investigations would be required to confirm this. Moreover, the light-dependent
13 cytotoxicity of **5** which is consistent with ROS-mediated apoptosis, was not observed for **4**,
14 and importantly, in the absence of light activation, complex **5** was found to be cleared from
15 the cells without causing any damage. In addition, compared to commercially available
16 porphyrins, which often consist of a mixture of products, complex **5** is pure. **5** can also be
17 easily modified and will be used to further refine the structure-activity relationship required
18 for even more potent PDT agents. Studies are also currently underway to develop analogues
19 of **5** which can be photoactivated by longer wavelengths of light to allow for even better
20 tissue penetration. It should be noted that while other investigators have described
21 mitochondrial uptake of Ru(II) based polypyridyl compounds^{18, 25, 39}, the vast majority of
22 these complexes are not photo-active, highlighting the novel importance of the current study.
23

24 In summary, complex **5** reveals it has promise for development as a new
25 photodynamic therapeutic. It is pure, hydrophilic, easily accumulates in cancer cells, has little
26 dark toxicity and clears the cells within 96 h, can be easily photoactivated, appears to have
27 high singlet oxygen production and can induce programmed cell death. The increased
28 understanding gained by a comprehensive biological profiling of the activity of this complex
29

1 brings us one step closer to the use of Ru(II) polypyridyl complexes to turn on cytotoxicity in
2 cancerous cells, and this has not been demonstrated in such a detailed manner before.
3
4
5
6

7 **Materials and Methods**
8

9 **Compounds:** Synthesis of Ru(II) polypyridyl complexes and ICP-MS sample preparation are
10 described in the Supplementary Information. All new compounds were characterised using
11 conventional methods (see full characterization in Supporting Information), which included
12 the use of 600 MHz NMR and elemental analysis (CHN) both of which confirmed that the
13 purity of all compounds made was over 95% (All ^1H and ^{13}C NMR spectra are shown in the
14 Supporting Information). Cell culture reagents were obtained from Greiner Bio-one and all
15 other chemicals were obtained from Sigma unless otherwise stated.
16
17
18
19
20
21
22
23
24
25
26

27 **Crystallographic Experimental Section:** Diffraction data for all compounds were collected
28 on a Bruker APEX 2 DUO CCD diffractometer using graphite-monochromatized Incoatec
29 $\text{I}\mu\text{S}$ Cu-K α ($\lambda = 1.54178 \text{ \AA}$) radiation. Crystals were mounted in a cryoloop/MiTeGen
30 micromount and collected at 100(2)K using an Oxford Cryosystems Cobra low temperature
31 device. Data were collected using omega and phi scans and were corrected for Lorentz and
32 polarization effects.²² The structures were solved by direct methods with SHELXS 2013 and
33 refined by full-matrix least-squares procedures on F^2 using SHELXL-2013 software.²⁴ All
34 non-hydrogen atoms were refined anisotropically. Hydrogen atoms, with the exception of
35 those of the water molecule, were added geometrically in calculated positions and refined
36 using a riding model. Hydrogen bond analysis was used to places the hydrogens of the water
37 molecule and their positions were kept fixed. Details of the data collection and refinement are
38 given in the supplementary information section. CCDC 1012983 contains the supplementary
39 crystallographic data for this paper. These data can be obtained free of charge from The
40 Cambridge Crystallographic Data Centre via www.ccdc.cam.ac.uk/data_request/cif.
41
42
43
44
45
46
47
48
49
50
51
52
53
54
55
56
57
58
59
60

1 **Agarose gel electrophoresis:** The DNA photocleavage studies were carried out by treating
2 pBR322 plasmid DNA (1 mg/mL) with each of the complexes at varying ratios (P/D 100,
3 50). The samples were then subjected to 2 J cm^{-2} using a Hamamatsu L2570 200 Watt HgXe
4 Arc Lamp equipped with a NaNO_2 filter before being separated using 0.8% agarose gel
5 electrophoresis in a TBE (90 mM Tris-borate, 2 mM EDTA, pH 8.0) buffer. Electrophoresis
6 was carried out at 5 V/cm (40 mA, 90 V). Visualisation of the DNA was achieved by staining
7 the gel for 90 mins with an aqueous solution of ethidium bromide, which was then
8 illuminated with a transilluminator (Bioblock 254 UV illuminator).

19
20
21 **Cell culture:** HeLa, ONE-58 and CRL5915 cells were grown in a cell culture flask using
22 low-glucose Dulbecco's Modified Eagle Medium supplemented with 10 % fetal bovine
23 serum and 50 $\mu\text{g}/\text{ml}$ penicillin/streptomycin at 37°C in a humidified atmosphere of 5% CO_2 .
24 MUTU-I and DG-75 cells were cultured in RPMI medium with supplements as listed above
25 however MUTU-I cells also required the addition of 1 mM HEPES, 100 mM sodium
26 pyruvate and 50 mM α -thioglycerol in PBS with 20 μM bathocuprione disulfonic acid. For
27 photoactivation studies, cells were subjected to 18 J cm^{-2} using a Hamamatsu L2570 200
28 Watt HgXe Arc Lamp equipped with a NaNO_2 filter.

29
30
31 **Viability assay:** For the alamar blue cytotoxicity test involving Ru (II) polypyridyl
32 complexes, $1-5 \times 10^3$ cells/well were seeded in a 96-well plate and treated with the respective
33 drug for 24 h \pm irradiation. After 24h, each well was then treated with 20 μl of Alamar Blue
34 (BioSource) (pre-warmed to 37°C) and left to incubate at 37°C in the dark for 4-6 h.
35 Fluorescence was read using at 590 nm (excitation 544 nm). The background fluorescence of
36 the media without cells + Alamar Blue was taken away from each group, and the control
37 untreated cells represented 100 % cell viability. Each compound was screened over a 1 μM -1
38 mM concentration range in triplicate on two independent days with activity expressed as
39 percentage cell viability compared to vehicle treated controls. All data points (expressed as
40

means \pm S.E.M.) were analysed using GRAPHPAD Prism (version 4) software (Graphpad software Inc., San Diego, CA).

Confocal microscopy: HeLa cells were seeded at a density of 0.75×10^5 cells /2 ml, left for 24 h before treating with **4** or **5** for the indicated length of time. Cells were washed X2 with new media to remove excess drug and analysed by live confocal microscopy using an Olympus FV1000 point scanning microscope with a 60x oil immersion lens with an NA (numerical aperture) of 1.42. The software used to collect images was FluoView Version 7.1 software. For temperature dependent uptake studies, cells were placed at 4°C for 30 min before treatment with **5** for 4 h at 4°C . Uptake was assessed at the fluorescence per cell at 600-700 nm, carried out on 300 cells on three independent days.. For the real-time confocal microscopy experiments with photoirradiation, treated cells were irradiated for 30 min and phase-contrast images were taken every ten min for 12 h.

Propidium Iodide staining: For the detection of apoptotic bodies by PI FACS analysis, 250,000 cells were treated with the appropriate amount of compound and incubated for a specified time. Cells were harvested by centrifugation at 300xg for 5 min and washed with 5ml of ice-cold PBS. The pellet was resuspended in 200 μl PBS and 2ml of ice-cold 70% ethanol and cells were fixed overnight at 4°C . After fixation, the cells were pelleted by centrifugation at 300xg for 5 min and the ethanol was carefully removed. The pellet was resuspended in 400 μl of PBS with 25 μl of RNase A (10mg/ ml stock) and 75 μl of propidium iodide (1mg/ml). The tubes were incubated in the dark at 37°C for 30 min. Cell cycle analysis was performed using appropriate gates counting 10,000 cells and analysed using CELLQUEST software package. For mechanistic studies, cells were pre-incubated with 40 μM z-VAD-fmk or 5 mM N-acetyl cysteine before treatment with **5**, irradiation and PI FACS analysis was then performed.

1 **Western blotting:** For the detection of PARP cleavage by Western Blot analysis 5×10^6 cells
2 were harvested by centrifugation at 500xg for 5 min and the pellet washed with ice-cold PBS.
3 Cells were resuspended in 60 μ l PBS and 60 μ l lysis buffer (Laemmli buffer; 62.5mM Tris-
4 HCl, 2 % w/v SDS, 10 % glycerol, 0.1 % w/v bromophenol blue supplemented with protease
5 inhibitors). Samples were prepared for SDS-PAGE resolved on an 8 % loading gel and
6 transferred onto PVDF membranes. Membranes were probed with anti-PARP (Calbiochem)
7 (recognizes full length 113 kDa PARP as well as the 85 kDa cleaved form) primary
8 antibody followed by incubation with the corresponding IgG HRP conjugated secondary
9 antibody. Membranes were developed using electrochemiluminescence detection.
10
11

21 **Colocalisation studies:** 0.3×10^5 HeLa cells were seeded, left for 24 h, and transfected with
22 an excitable (405 nm)-GFP mitochondrial/lysosomal or CFP-tagged ER marker. After 24 h,
23 cells were treated with **5** (100 μ M) for 16 h, washed twice with fresh media and analysed by
24 live confocal microscopy. The sample was first excited with a 488 nm laser diode and the
25 emission of drug was monitored and captured at 600-700 nm. The sample was then excited
26 with a 405 nm laser diode (GFP) or a Green Helium-Neon laser (CFP) and the emission of
27 the excitable marker was monitored and captured at 495-550 nm (GFP) or 470-500 nm
28 (CFP). Both images were then overlaid and analysed using the Imaris 3D software analyser
29 (Bitplane).
30
31

42 **Membrane potential:** HeLa cells incubated for the required times with Ru (II) complexes
43 followed by the addition of a final concentration of 5 nM TPMP, 100 nCi/ml [3 H]TPMP and
44 5 nM sodium tetraphenylboron (TPB) for 90 min with or without 1 μ M FCCP. After
45 incubation, the cells were pelleted by centrifugation, 100 μ l of the supernatant was removed
46 and the cell pellet resuspended in 100 μ l 20% Triton X-100. The radioactivity in the pellet
47 and supernatant was quantitated using a liquid scintillation counter with appropriate quench
48 corrections. Accumulation ratio = cpm/mg (pellet) : cpm/ μ l (supernatant). MMP =
49 Accumulation ratio without FCCP – Accumulation ratio with FCCP.
50
51
52
53
54
55
56
57
58
59
60

1
2 **Transmission electron microscopy:** Was carried out as previously described⁵³. In brief,
3 1x10⁶ cells were treated with 100 µM of **5** for 24 h, fixed with 4% glutaraldehyde for 1 h,
4 washed in 0.5 M phosphate, solidified in 2% warm agarose solution at 4 °C for 30 min and
5 cut into small slices. Slices were further fixed in 2% osmium tetroxide (O₂O₄) solution in
6 0.05 M potassium phosphate buffer and dehydrated using an increasing alcohol series. Pellets
7 were embedded in a 50% resin solution for 2–3 h and a 100% epoxy. Ultrathin sections were
8 cut on an ultramicrotome and collected on copper grids and counterstained with uranyl
9 acetate and lead citrate. Ultrastructural examination was carried out in a JOEL 1210 electron
10 microscope. Images were taken with a 1,500–3,000X objective (2 µM scale bars). A number
11 of images were obtained as a representative of each sample.
12
13
14
15
16
17
18
19
20
21
22
23
24
25
26
27
28
29
30
31
32
33
34
35
36
37
38
39
40
41
42
43
44
45
46
47
48
49
50
51
52
53
54
55
56
57
58
59
60

Comet assay: HeLa cells were treated with 10 µM **4** or 20 µM **5** for 24 h ± irradiation and incubated for a further 6 h. Following which, cells were trypsinised and resuspended in low melting point agarose (LMPA) and added to slides pre-coated with normal melting point agarose (NPA). Slides were then lysed (2.5 M NaCl, 100 mM EDTA, 10 mM Tris, 1% (v/v) Triton X-100, pH 10) for 2 h at -20 °C and transferred to an alkaline buffer (300 mM NaOH, 1 mM EDTA, pH >13) for 20 min to allow for unwinding of DNA and expression of alkali-labile damage. Slides were then subjected to electrophoresis at 24 V, 300 mA for 30 min. Samples were then neutralised in 0.4 M Tris, pH 7.5 for 20 min and stained with PI. Slides were viewed using an Olympus IX81 microscope with a 20x lens. The software Cell^{^P} was used to collect images.

Statistical analysis: Data was analysed with the software Prism GraphPad using a one-way ANOVA. For illustrative purposes the p values are presented as *, p < 0.05.

1 † The initial addition of st-DNA (P/D 0-4) resulted in an immediate fluorescence increase,
2 however, upon further addition of st-DNA (P/D 0-20) the emission spectrum of **4** exhibited a
3 decrease in photoluminescence with no changes being observed thereafter. We attribute this
4 behaviour to biphasic interactions in which these bulky complexes are initially efficiently
5 packed along the DNA helix providing increased shelter from solvent quenching resulting in
6 increased fluorescence compared to the isolated complexes along the helix. This is similar
7 behaviour that has been seen for related systems^{54, 55}. Similar behaviour is observed with
8 DNA homopolymers, however, the initial fluorescence intensity is increased upon interaction
9 with [poly(dA-dT)]₂.

10
11 §Further titrations using the homopolymers [poly(dA-dT)]₂ and [poly(dG-dC)]₂ revealed that
12 significant discrimination was observed for both complexes, whereby, **4** showed superior
13 binding affinity with $K = 1.8 \times 10^7 \text{ M}^{-1}$ (± 0.4) and $n = 1.71$ (± 0.02) for [poly(dA-dT)]₂ and
14 $K = 8.0 \times 10^6 \text{ M}^{-1}$ (± 0.4) and $n = 1.54$ (± 0.08) for [poly(dG-dC)]₂. Similarly, **5** bound
15 to [poly(dA-dT)]₂ with $K = 1.1 \times 10^7 \text{ M}^{-1}$ (± 0.17) and $n = 1.85$ (± 0.02) while the binding of **5**
16 to [poly(dG-dC)]₂ gave $K = 3.77 \times 10^6 \text{ M}^{-1}$ (± 0.2) and $n = 1.33$ (± 0.01). (A full table of
17 binding constants and binding site stoichiometries is available in Supplementary Information)

ASSOCIATED CONTENT

18
19 **Supporting Information.** This material is available free of charge via the Internet at
20
21 <http://pubs.acs.org>

AUTHOR INFORMATION

Corresponding Author

22 Correspondence and request for material should be addressed to DCW; E-mail:
23 clive.williams@tcd.ie; Fax: +353 1 8963130; Tel: +353 1 8963964 and TG E-mail:
24 gunnlaut@tcd.ie; Fax: +353 1 6712826, Tel: +353 1 8963459.

1
2
Author Contributions
3
4
5
6
7
8

The manuscript was written through contributions of all authors. All authors have given approval to the final version of the manuscript. ‡These authors contributed equally.

9
10
ACKNOWLEDGMENT
11
12
13
14
15
16
17
18

We thank Science Foundation Ireland (SFI RFP 2009, SFI 2010 PI and 2013 PI grants), HEA PRTLI Cycle 4, The Irish Research Council for Science, Engineering and Technology (IRCSET Postgraduate Studentship to RPBE), Master and Back Altaformazione Programma, 2009, Autonomous Region of Sardinia and TCD for financial support.

19
20
21
22
ABBREVIATIONS
23
24
25
26
27
28
29
30
31
32
33
34
35
36
37

dppz, dipyrido[3,2-a:2',3'-c]phenazine; FACS, fluorescent activated cell sorter; LD, Linear Dichroism; MCLT, Metal charge to ligand transfer; MMP, mitochondrial membrane potential; NAC, *N*-acetyl cysteine; TAP, tetraazaphenanthrene; TEM, Transmission electron microscopy, pdppz, ([2, 3-h]dipyrido[3,2-a:2',3'-c]phenazine; PDT, photodynamic therapy; phen, 1,10-phenanthroline; PI, propidium iodide; ROS, reactive oxygen species; stDNA, salmon testes DNA.

38
39
40
REFERENCES
41
42
43
44
45
46
47
48
49

1. (a) Combination of Ru(II) complexes and light: new frontiers in cancer therapy, Mari,C.; Pierroz,V.; Ferrari, S.; Gasser, G. *Chem. Sci.* **2015**, DOI: 10.1039/C4SC03759F. (b) Vos, J. G.; Kelly, J. M. Ruthenium polypyridyl chemistry; from basic research to applications and back again. *Dalton Trans.* **2006**, 4869-4883.
2. Schäfer, S.; Ott, I.; Gust, R.; Sheldrick, W. S. Influence of the Polypyridyl (pp) Ligand Size on the DNA Binding Properties, Cytotoxicity and Cellular Uptake of Organoruthenium(II) Complexes of the Type $[(\eta^6\text{-C}_6\text{Me}_6)\text{Ru(L)(pp)}]^{n+}$ [L = Cl, n = 1; L = (NH₂)₂CS, n = 2]. *Eur J Inorg Chem.* **2007**, 3034–3046.

- 1 3. Pisani, M. J.; Weber, D. K.; Heimann, K.; Collins, J. G.; Keene, F. R. Selective mitochondrial
2 accumulation of cytotoxic dinuclear polypyridyl ruthenium(II) complexes. *Metallomics* **2010**, 2, 393-
3 396.
- 4 4. Huang, H.; Zhang, P.; Yu, B.; Chen, Y.; Wang, J.; Ji, L.; Chao, H. Targeting Nucleus DNA with a
5 Cyclometalated Dipyridophenazineruthenium(II) Complex. *J Med Chem.* **2014**, 57, 8971-8983.
- 6 5. Niyazi, H.; Hall, J. P.; O'Sullivan, K.; Winter, G.; Sorensen, T.; Kelly, J. M.; Cardin, C. J. Crystal
7 structures of Lambda-[Ru(phen)(2)dppz](2+) with oligonucleotides containing TA/TA and AT/AT
8 steps show two intercalation modes. *Nat Chem.* **2012**, 4, 621-628.
- 9 6. Nonat, A. M.; Quinn, S. J.; Gunnlaugsson, T. Mixed f-d Coordination Complexes as Dual
10 Visible- and Near-Infrared-Emitting Probes for Targeting DNA. *Inorg Chem.* **2009**, 48, 4646-4648.
- 11 7. Ryan, G. J.; Quinn, S.; Gunnlaugsson, T. Highly Effective DNA Photocleavage by Novel "Rigid"
12 Ru(bpy)3-4-nitro- and -4-amino-1,8-naphthalimide Conjugates. *Inorg Chem.* **2008**, 47, 401-403.
- 13 8. Zeglis, B. M.; Pierre, V. C.; Barton, J. K. Metallo-intercalators and metallo-insertors. *Chem*
14 _{Commun (Camb).} **2007**, 4565-4579.
- 15 9. Moucheron, C.; Kirsch-De Mesmaeker, A.; Kelly, J. M. Photoreactions of ruthenium(II) and
16 osmium(II) complexes with deoxyribonucleic acid (DNA). *J Photochem Photobiol B.* **1997**, 40, 91-106.
- 17 10. Erkkila, K. E.; Odom, D. T.; Barton, J. K. Recognition and reaction of metallointercalators with
18 DNA. *Chem Rev.* **1999**, 99, 2777-2795.
- 19 11. Song, H.; Kaiser, J. T.; Barton, J. K. Crystal structure of Delta-[Ru(bpy)(2)dppz](2+) bound to
20 mismatched DNA reveals side-by-side metalloinsertion and intercalation. *Nat Chem.* **2012**, 4, 615-
21 620.
- 22 12. Gill, M. R.; Thomas, J. A. Ruthenium(II) polypyridyl complexes and DNA-from structural
23 probes to cellular imaging and therapeutics. *Chem Soc Rev.* **2012**, 41, 3179-3192.
- 24 13. Elmes, R. B.; Orange, K. N.; Cloonan, S. M.; Williams, D. C.; Gunnlaugsson, T. Luminescent
25 ruthenium(II) polypyridyl functionalized gold nanoparticles; their DNA binding abilities and
26 application as cellular imaging agents. *J Am Chem Soc.* **2011**, 133, 15862-15865.

- 1 14. Elmes, R. B.; Erby, M.; Bright, S. A.; Williams, D. C.; Gunnlaugsson, T. Photophysical and
2 biological investigation of novel luminescent Ru(II)-polypyridyl-1,8-naphthalimide Troger's bases as
3 cellular imaging agents. *Chem Commun (Camb)*. **2012**, 48, 2588-2590.
- 4 15. Kelly, J. M.; McConnell, D. J.; Ohuigin, C.; Tossi, A. B.; Kirsch-De Mesmaeker, A.; Masschelein,
5 A.; Nasielski, J. Ruthenium Polypyridyl Complexes - Their Interaction with DNA and Their Role as
6 Sensitizers for Its Photocleavage. *J Chem Soc Chem Commun*. **1987**, 1821-1823.
- 7 16. Elias, B.; Creely, C.; Doorley, G. W.; Feeney, M. M.; Moucheron, C.; Kirsch-De Mesmaeker, A.;
8 Dyer, J.; Grills, D. C.; George, M. W.; Matousek, P.; Parker, A. W.; Towrie, M.; Kelly, J. M.
9 Photooxidation of Guanine by a Ruthenium Dipyridophenazine Complex Intercalated in a Double-
10 Stranded Polynucleotide Monitored Directly by Picosecond Visible and Infrared Transient Absorption
11 Spectroscopy. *Chemistry* **2007**, 14, 369-375.
- 12 17. Herman, L.; Ghosh, S.; Defrancq, E.; Kirsch-De Mesmaekera, A. Ru(II) complexes and light:
13 molecular tools for biomolecules. *J Phys Org Chem*. **2008**, 21, 670-681.
- 14 18. Puckett, C. A.; Barton, J. K. Methods to explore cellular uptake of ruthenium complexes. *J Am
15 Chem Soc*. **2007**, 129, 46-47.
- 16 19. Allison, R. R.; Bagnato, V. S.; Sibata, C. H. Future of oncologic photodynamic therapy. *Future
17 Oncol*. **2010**, 6, 929-940.
- 18 20. O'Connor, A. E.; Gallagher, W. M.; Byrne, A. T. Porphyrin and nonporphyrin photosensitizers
19 in oncology: preclinical and clinical advances in photodynamic therapy. *Photochem Photobiol*. **2009**,
20 85, 1053-1074.
- 21 21. Triesscheijn, M.; Baas, P.; Schellens, J. H. M.; Stewart, F. A. Photodynamic Therapy in
22 Oncology. *Oncologist*. **2006**, 11, 1034-1044.
- 23 22. Keane, P. M.; Poynton, P. E.; Hall, J. P.; Clark, I. P.; Sazanovich, I. V.; Towrie, M.; Gunnlaugsson,
24 T.; Quinn, S. J.; Cardin, C. J.; Kelly, J. M. Enantiomeric Conformation Controls Rate and Yield of
25 Photoinduced Electron Transfer in DNA Sensitized by Ru(II) Dipyridophenazine Complexes. *J. Phys.
26 Chem. Lett.* **2015**, 6, 734-738.

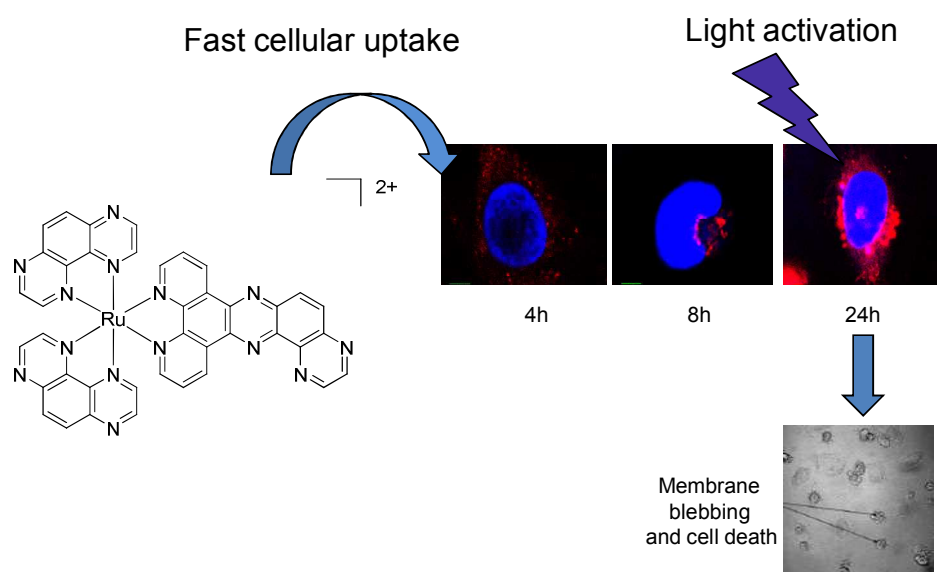
- 1 23. Ortmans, I.; Elias, B.; Kelly, J. M.; Moucheron, C.; Kirsch-De Mesmaeker, A.
2 [Ru(TAP)2(dppz)]2+: a DNA intercalating complex, which luminesces strongly in water and undergoes
3 photo-induced proton-coupled electron transfer with guanosine-5'-monophosphate. *Dalton Trans.*
4
5 2004, 4, 668-676.
- 6
7 24. Sheldrick, G. M. SHELXL-2013. **2013**.
- 8
9 25. Dickerson, M.; Sun, Y.; Howerton, B.; Glazer, E. C. Modifying Charge and Hydrophilicity of
10 Simple Ru(II) Polypyridyl Complexes Radically Alters Biological Activities: Old Complexes, Surprising
11 New Tricks. *Inorg Chem.* **2014**, 53, 10370-10377.
- 12
13 26. Gill, M. R.; Garcia-Lara, J.; Foster, S. J.; Smythe, C.; Battaglia, G.; Thomas, J. A. A ruthenium(II)
14 polypyridyl complex for direct imaging of DNA structure in living cells. *Nat Chem.* **2009**, 1, 662-667.
- 15
16 27. Cosgrave, L.; Devocelle, M.; Forster, R. J.; Keyes, T. E. Multimodal cell imaging by ruthenium
17 polypyridyl labelled cell penetrating peptides. *Chem Commun (Camb)*. **2010**, 46, 103-105.
- 18
19 28. Puckett, C. A.; Barton, J. K. Targeting a ruthenium complex to the nucleus with short
20 peptides. *Bioorg Med Chem.* **2010**, 18, 3564-3569.
- 21
22 29. Puckett, C. A.; Barton, J. K. Fluorescein redirects a ruthenium-octaarginine conjugate to the
23 nucleus. *J Am Chem Soc.* **2009**, 131, 8738-8739.
- 24
25 30. Abrams, M. J. Novel water soluble agents for photodynamic cancer therapy. *Platinum Metals*
26 *Rev.* **1995**, 39, 14-18.
- 27
28 31. Elmes, R. B.; Erby, M.; Cloonan, S. M.; Quinn, S. J.; Williams, D. C.; Gunnlaugsson, T.
29 Quaternarized pdppz: synthesis, DNA-binding and biological studies of a novel dppz derivative that
30 causes cellular death upon light irradiation. *Chem Commun (Camb)*. **2011**, 47, 686-688.
- 31
32 32. Jacquet, L.; Davies, R. J. H.; Kirsch-De Mesmaeker, A.; Kelly, J. M. Photoaddition of
33 Ru(tap)2(bpy)2+ to DNA: A New Mode of Covalent Attachment of Metal Complexes to Duplex
34 DNA. *J Am Chem Soc.* **1997**, 119, 11763-11768.
- 35
36 33. Feeney, M. M.; Kelly, J. M.; Tossi, A. B.; Kirsch-De Mesmaeker, A.; Lecomte, J. P.
37 Photoaddition of Ruthenium(II)-Tris-1,4,5,8-Tetraazaphenanthrene to DNA and Mononucleotides. *J*
38 *Photochem Photobiol B.* **1994**, 23, 69-78.

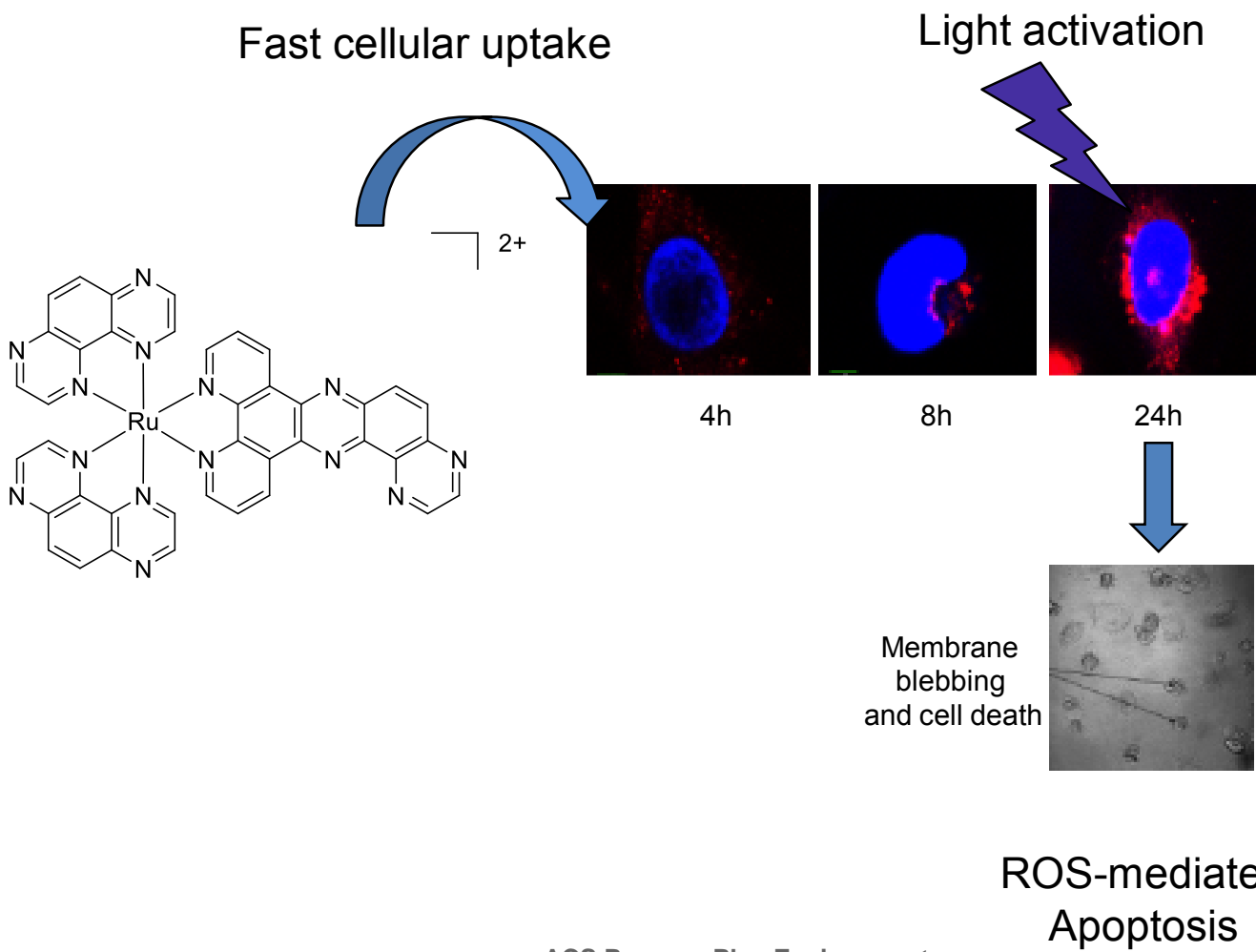
- 1 34. Nasielski-Hinkens, R.; Benedek-Vamos, M.; Maetens, D. Synthesis of 9-substituted 1,4,5,8
2 tetraazaphenanthrenes. *J. Heterocyclic Chem.* **1980**, *17*, 873-876.
- 3 35. Calucci, L.; Pampaloni, G.; Pinzino, C.; Prescimone, A. Transition metal derivatives of 1,10-
4 phenanthroline-5,6-dione: Controlled growth of coordination polynuclear derivatives. *Inorg. Chim.
5 Acta* **2006**, *359*, 3911-3920.
- 6 36. Rau, S.; Schäfer, B.; Grüßing, A.; Schebesta, S.; Lamm, K.; Vieth, J.; Görls, H.; Walther, D.;
7 Rudolph, M.; Grummt, U. W.; Birkner, E. Efficient synthesis of ruthenium complexes of the type (R-
8 bpy)2RuCl2 and [(R-bpy)2Ru(L-L)]Cl2 by microwave-activated reactions (R: H, Me, tert-But) (L-L:
9 substituted bibenzimidazoles, bipyrimidine, and phenanthroline). *Inorganica Chimica Acta* **2004**,
10 357, 4496-4503.
- 11 37. Carter, M. T.; Rodriguez, M.; Bard, A. J. Voltammetric studies of the interaction of metal
12 chelates with DNA. 2. Tris-chelated complexes of cobalt(III) and iron(II) with 1,10-phenanthroline
13 and 2,2'-bipyridine. *J Am Chem Soc.* **1989**, *111*, 8901–8911.
- 14 38. Lecomte, J. P.; Kirsch-De Mesmaeker, A.; Feeney, M. M.; Kelly, J. M. Ruthenium(II)
15 Complexes with 1,4,5,8,9,12-Hexaazatriphenylene and 1,4,5,8-Tetraazaphenanthrene Ligands: Key
16 Role Played by the Photoelectron Transfer in DNA Cleavage and Adduct Formation. *Inorg. Chem.*
17 **1995**, *34*, 6481-6491.
- 18 39. Chen, T.; Liu, Y.; Zheng, W. J.; Liu, J.; Wong, Y. S. Ruthenium polypyridyl complexes that
19 induce mitochondria-mediated apoptosis in cancer cells. *Inorg. Chem.* **2010**, *49*, 6366-6368.
- 20 40. Vollano, J. F.; Bossard, G. E.; Martellucci, S. A.; Darkes, M. C.; Abrams, M. J.; Brooks, R. C. The
21 synthesis and in vitro photodynamic activity of a series of novel ruthenium(II)-2,3-
22 naphthalocyanines. *J Photochem Photobiol B.* **1997**, *37*, 230-235.
- 23 41. Gallagher, W. M.; Allen, L. T.; O'Shea, C.; Kenna, T.; Hall, M.; Gorman, A.; Killoran, J.; O'Shea,
24 D. F. A potent nonporphyrin class of photodynamic therapeutic agent: cellular localisation, cytotoxic
25 potential and influence of hypoxia. *Br J Cancer* **2005**, *92*, 1702-1710.
- 26 42. Byrne, A. T.; O'Connor, A. E.; Hall, M.; Murtagh, J.; O'Neill, K.; Curran, K. M.; Mongrain, K.;
27 Rousseau, J. A.; Lecomte, R.; McGee, S.; Callanan, J. J.; O'Shea, D. F.; Gallagher, W. M. Vascular-
28

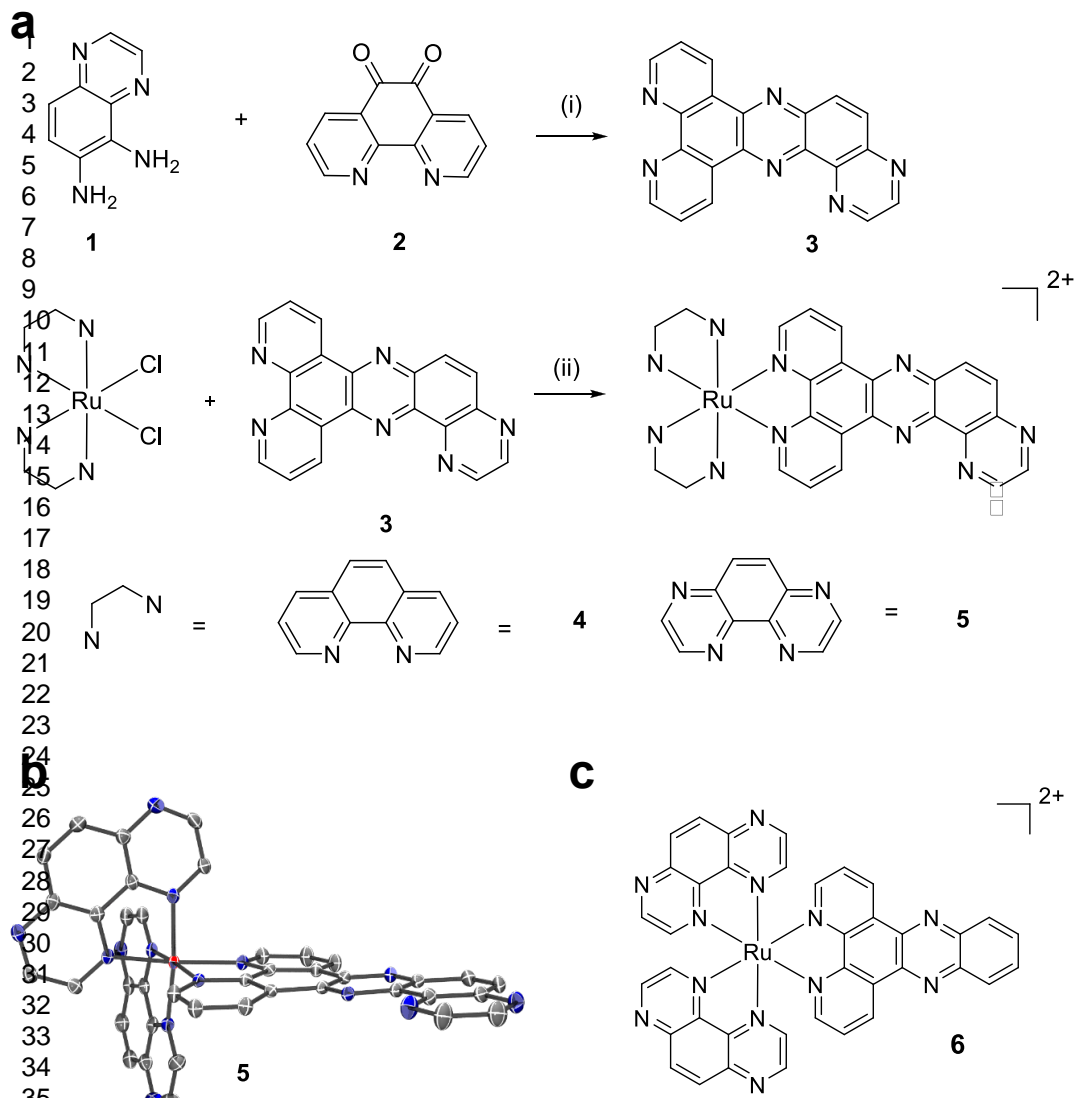
- targeted photodynamic therapy with BF2-chelated Tetraaryl-Azadipyrromethene agents: a multi-modality molecular imaging approach to therapeutic assessment. *Br J Cancer* **2009**, 101, 1565-1573.
43. Gauthier, N.; De Winter, J.; Gerbaux, P.; Moucheron, C.; Luhmer, M.; Kirsch-De Mesmaeker, A. A Ru(II)-TAP complex, photoreagent for tryptophan-containing peptides: structure of the covalent photoadduct. *Inorg Chem.* **2010**, 49, 6796-6798.
44. Rickling, S.; Ghisdavu, L.; Pierard, F.; Gerbaux, P.; Surin, M.; Murat, P.; Defrancq, E.; Moucheron, C.; Kirsch-De Mesmaeker, A. A Rigid Dinuclear Ruthenium(II) Complex as an Efficient Photoactive Agent for Bridging Two Guanine Bases of a Duplex or Quadruplex Oligonucleotide. *Chemistry* **2010**, 16, 3951-3961.
45. Zhang J; Wong KL; Wong WK; Mak NK; Kwong DW; HL., T. Two-photon induced luminescence, singlet oxygen generation, cellular uptake and photocytotoxic properties of amphiphilic Ru(II) polypyridyl-porphyrin conjugates as potential bifunctional photodynamic therapeutic agents. *Org Biomol Chem.* **2011**, 9, 6004-6010.
46. Poon CT; Chan PS; Man C; Jiang FL; Wong RN; Mak NK; Kwong DW; Tsao SW; WK., W. An amphiphilic ruthenium(II)-polypyridyl appended porphyrin as potential bifunctional two-photon tumor-imaging and photodynamic therapeutic agent. *J Inorg Biochem.* **2010**, 104, 62-70.
47. Xu, W.; Zuo, J.; Wang, L.; Jia, L.; Chao, H. Dinuclear ruthenium(II) polypyridyl complexes as single and two-photon luminescence cellular imaging probes. *Chem. Commun.* **2014**, 50, 2123-2125.
48. Cetinbas, N.; Webb, M. I.; Dubland, J. A.; Walsby, C. J. Serum-protein interactions with anticancer Ru(III) complexes KP1019 and KP418 characterized by EPR. *J. Biol. Inorg. Chem* **2010**, 15, 131-145.
49. Levina, A.; Mitra, A.; P.A., L. Recent developments in ruthenium anticancer drugs. *Metalomics*. **2009**, 1, 458-470.
50. Pernot, M.; Bastogne, T.; Barry, N. P.; Therrien, B.; Koellensperger, G.; Hann, S.; Reshetov, V.; Barberi-Heyob, M. Systems biology approach for in vivo photodynamic therapy optimization of ruthenium-porphyrin compounds. *J Photochem Photobiol B*. **2012**, 117, 80-89.

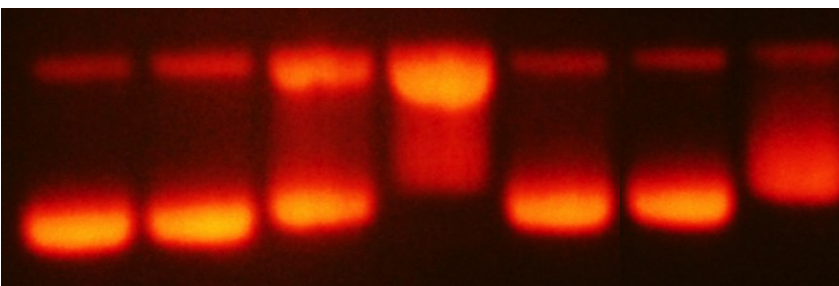
- 1 51. Puckett, C. A.; Barton, J. K. Mechanism of cellular uptake of a ruthenium polypyridyl
2 complex. *Biochemistry*. **2008**, *47*, 11711-11716.
- 3
- 4 52. Youle, R. J.; Narendra, D. P. Mechanisms of mitophagy. *Nat Rev Mol Cell Biol*. **2011**, *12*, 9-14.
- 5
- 6 53. Cloonan, S. M.; Williams, D. C. The antidepressants maprotiline and fluoxetine induce Type II
7 autophagic cell death in drug-resistant Burkitt's lymphoma. *Int J Cancer*. **2011**, *128*, 1712-1723.
- 8
- 9
- 10 54. Moucheron, C.; Kirsch-De Mesmaeker, A.; Choua, S. Photophysics of Ru(phen)2(PHEHAT)2⁺:
11 A Novel Light Switch for DNA and Photo-oxidant for Mononucleotides. *Inorg Chem*. **1997**, *36*, 584-
12
- 13 592.
- 14
- 15 55. Hiort, C.; Lincoln, P.; Norden, B. DNA binding of .DELTA.- and .LAMBDA.-[Ru(phen)2DPPZ]2⁺.
16 *J Am Chem Soc*. **1993**, *115*, 3448-3454.
- 17
- 18
- 19
- 20
- 21
- 22
- 23
- 24
- 25
- 26
- 27
- 28
- 29
- 30
- 31
- 32
- 33
- 34
- 35
- 36
- 37
- 38
- 39
- 40
- 41
- 42
- 43
- 44
- 45
- 46
- 47
- 48
- 49
- 50
- 51
- 52
- 53
- 54
- 55
- 56
- 57
- 58
- 59
- 60

Table Of Contents Graphic

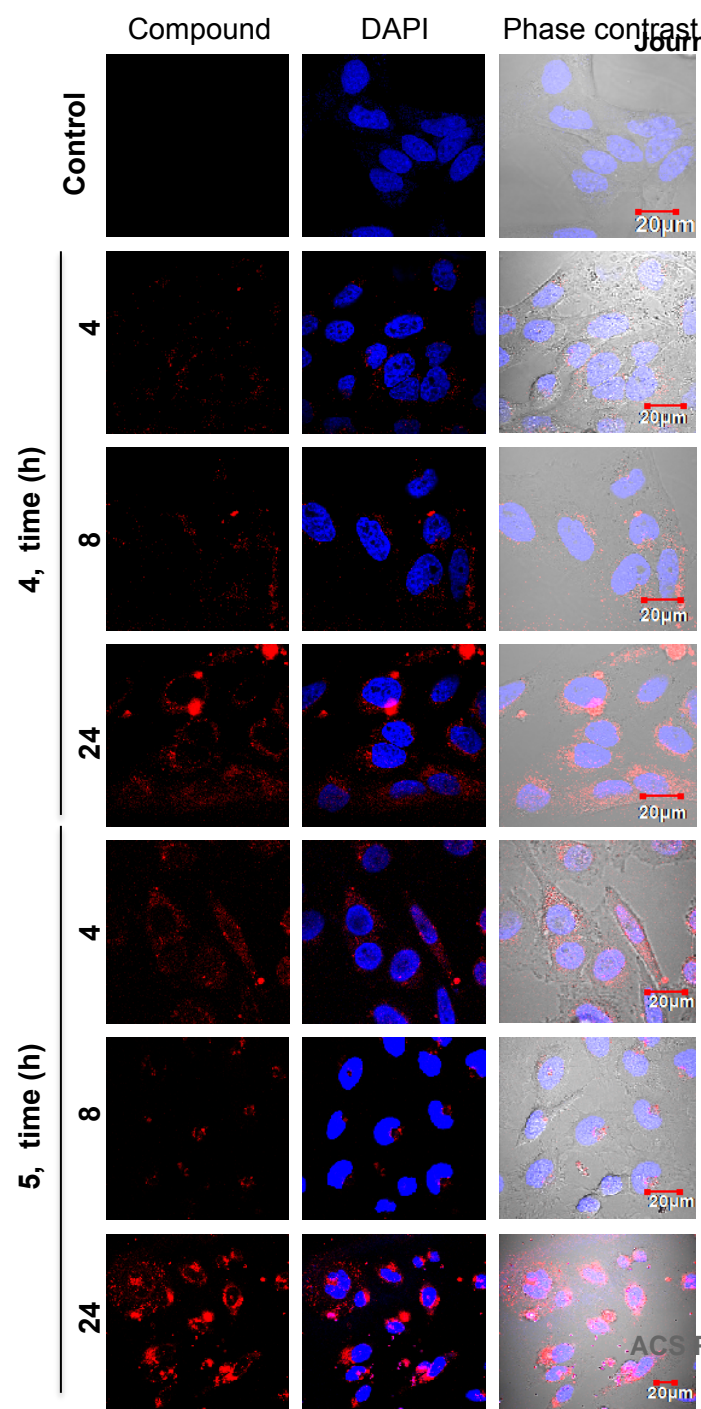
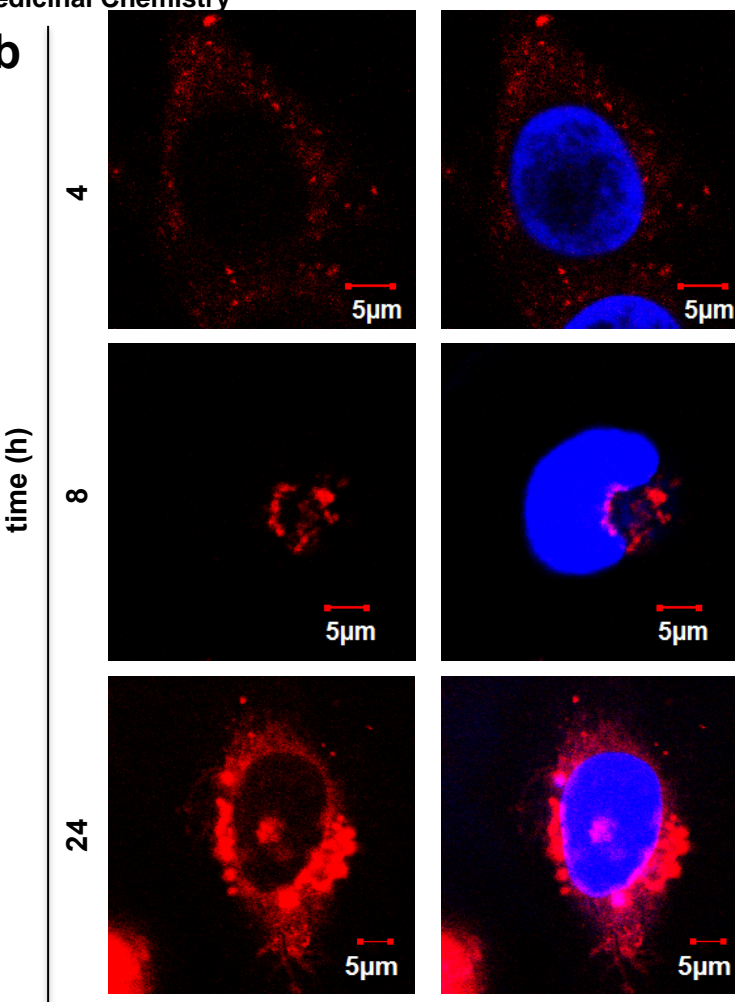
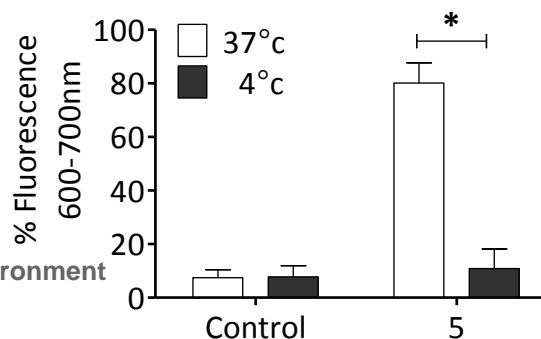


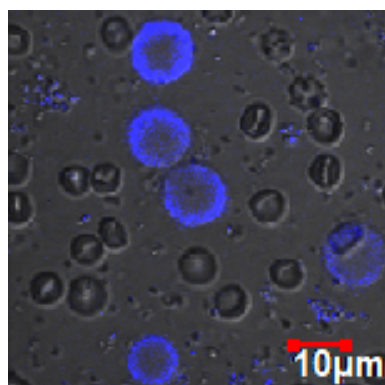
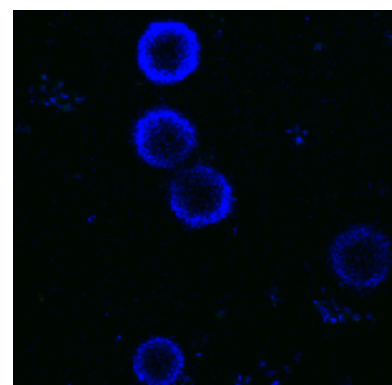






1 2 3 4 5 6 7

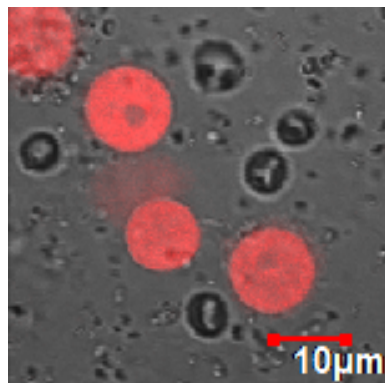
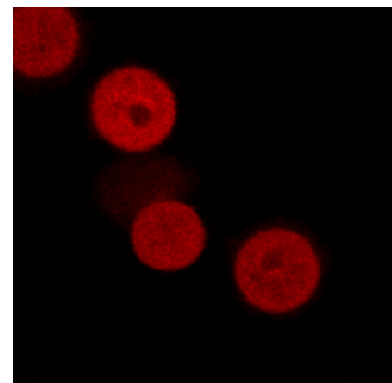
a**b****c**



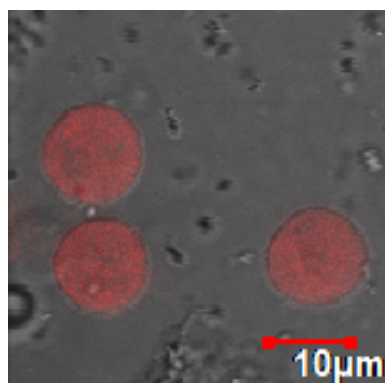
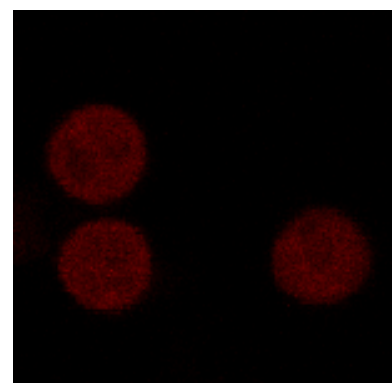
b

Ru (II) compound

Phase contrast

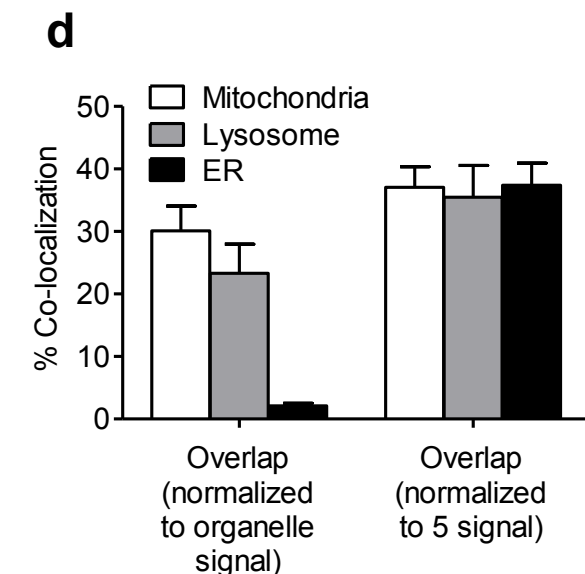
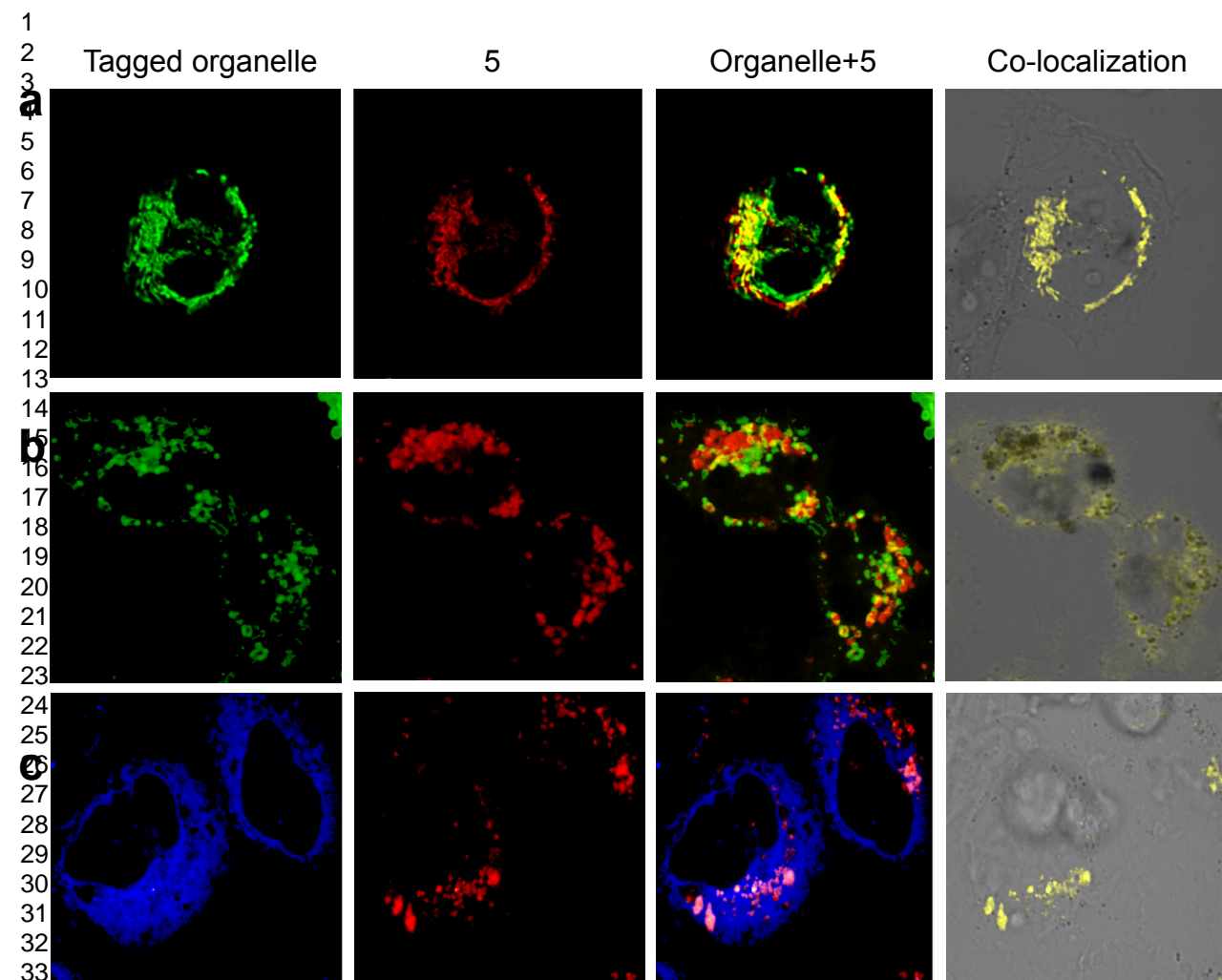


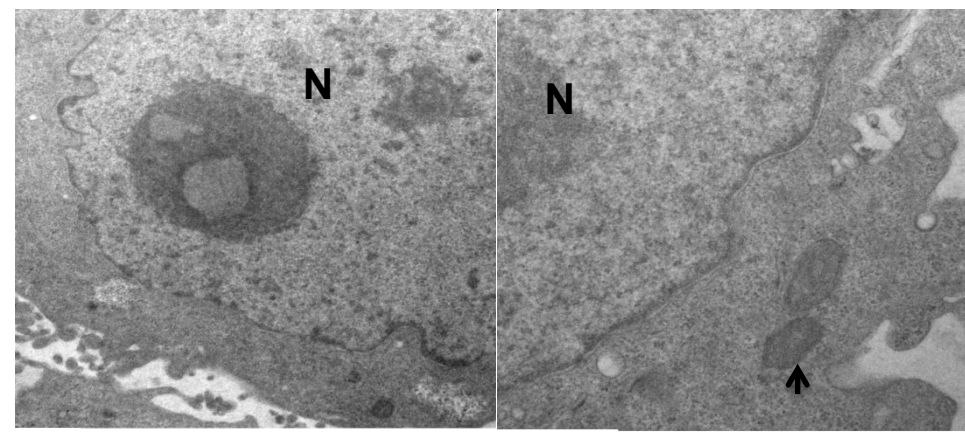
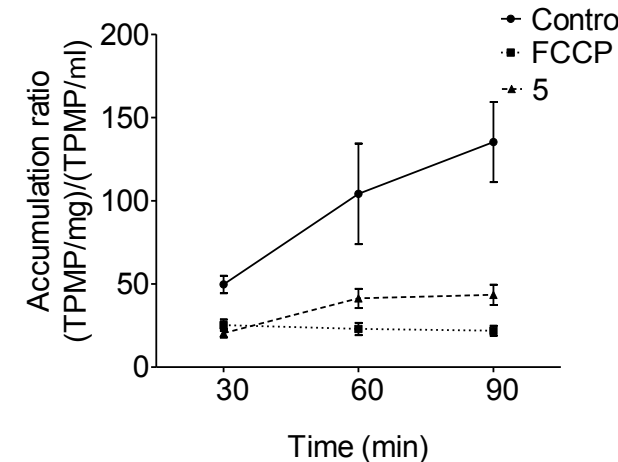
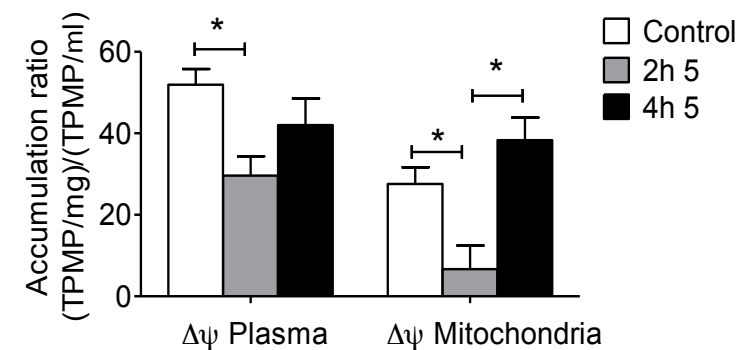
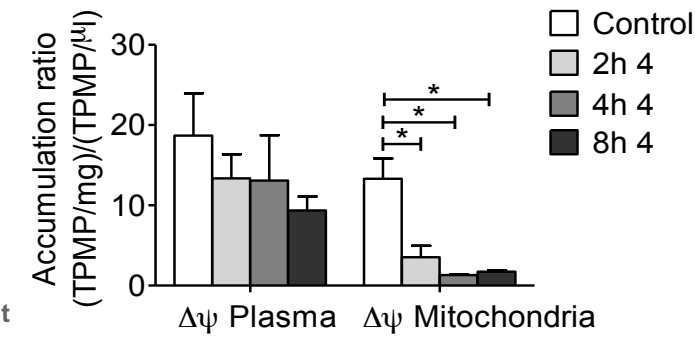
4



5

ACS Paragon Plus Environment



a**b****c****d**

5

